

# Matrix denoising for weighted loss functions and heterogeneous signals

William Leeb

## Abstract

We consider the problem of recovering a low-rank matrix from a noisy observed matrix. Previous work has shown that the optimal method for recovery depends crucially on the choice of loss function. We use a family of weighted loss functions, which arise naturally in many settings such as heteroscedastic noise and missing data. Weighted loss functions are challenging to analyze because they are not orthogonally-invariant. We derive optimal spectral denoisers for these weighted loss functions. By combining different weights, we then use these optimal denoisers to construct a new denoiser that exploits heterogeneity in the signal matrix for more accurate recovery with unweighted loss.

## 1 Introduction

This paper is concerned with the problem of matrix denoising: estimating a low-rank signal matrix  $\mathbf{X}$  from an observed matrix  $\mathbf{Y} = \mathbf{X} + \mathbf{G}$ , where  $\mathbf{G}$  is a full-rank matrix of noise. Our starting point will be a popular and well-studied technique for this problem, known as *singular value shrinkage* [50, 19, 18, 45, 17]. In its simplest incarnation, singular value shrinkage keeps the singular vectors of the observed matrix  $\mathbf{Y}$ , while deflating its singular values to remove the effects of the noise. Most of the observed singular values will be set to 0, while ideally the top  $r$  singular values (if  $\mathbf{X}$  has rank  $r$ ) will be modified by a certain amount to remove the influence of the noise.

The assumption that the target matrix  $\mathbf{X}$  is low-rank is sometimes referred to as the *spiked model* [2, 1, 4, 46, 31, 6]. Often,  $\mathbf{X}$  is modelled as a random matrix with iid columns drawn from a low-rank population covariance matrix, though in the present paper we will not assume that  $\mathbf{X}$  is random; we describe our precise observation model in Section 1.1. The spiked model is typically studied in the *high-dimensional* asymptotic regime. This is where the number of rows and columns of  $\mathbf{X}$  grow proportionally to each other; that is, if  $\mathbf{X}$  has  $p$  rows and  $n$  columns, we assume both  $p$  and  $n$  grow to infinity, and their ratio  $p/n$  converges to a definite limit.

This paper will address two apparent gaps in the present understanding of the class of singular value shrinkage estimators. First, we will extend the range of loss functions with which this class of methods may be applied. In particular, we study the class of *weighted* loss functions, in which errors in different rows and columns incur different penalties. As we will explain in Section 2, these loss functions arise naturally in a number of applications, such as denoising with heteroscedastic noise [41, 58] and in the presence of missing data and other linear deformations of  $\mathbf{X}$  [14]. However, weighted loss functions are mathematically challenging because they are not orthogonally invariant. We extend the theory we introduced in [41] to derive optimal spectral estimators for a class of weighted loss functions.

The second main topic of this paper is the question of when singular value shrinkage is optimal, even for unweighted loss. Prior work has shown that when the noise matrix  $\mathbf{G}$  is orthogonally-invariant, then for orthogonally-invariant loss functions singular value shrinkage is both minimax optimal [17] and optimal in expectation over a uniform prior on the signal singular vectors [50]. More informally, singular value shrinkage is optimal when we possess no prior knowledge on the signal. This leaves open the question of how to exploit structural information on the signal components. As a byproduct of our analysis of weighted loss functions, we derive a new matrix denoising algorithm for ordinary, unweighted Frobenius loss that is never worse than shrinkage, but may be significantly better. We call this method *localized denoising*. Localized denoising exploits *heterogeneity* in  $\mathbf{X}$ 's singular vectors. Informally, this means that when certain blocks of coordinates of  $\mathbf{X}$  are larger than others, localized denoising will outperform shrinkage.

The remainder of the paper is organized as follows. The rest of Section 1 introduces the observation model, describes the class of methods we will study and the main results, and makes comparisons to previous works. Section 2 examines two problems where weighted loss functions are naturally used, specifically missing data problems and heteroscedastic noise. Section 3 develops the new mathematical machinery we will use to derive optimal spectral denoisers for weighted loss. Section 4 derives these spectral denoisers in detail, and examines the optimal singular values as functions of the population and observed singular values. Section 5 introduces the aforementioned localized denoisers, and compares them to other procedures. Section 6 presents several numerical results, and Section 7 offers a summary and proposes topics for further study.

## 1.1 The observation model

We observe a  $p$ -by- $n$  data matrix  $\mathbf{Y} = \mathbf{X} + \mathbf{G}$ , consisting of a low-rank signal matrix  $\mathbf{X}$  and a full-rank isotropic Gaussian noise matrix  $\mathbf{G}$ . We will suppose  $\mathbf{X}$  is of the form:

$$\mathbf{X} = \sum_{k=1}^r t_k \mathbf{u}_k \mathbf{v}_k^T, \quad (1)$$

where the  $\mathbf{u}_k$  and  $\mathbf{v}_k$  are orthonormal vectors in  $\mathbb{R}^p$  and  $\mathbb{R}^n$ , respectively, and  $t_1 > \dots > t_r > 0$ . The entries of the noise matrix  $\mathbf{G}$  are iid  $N(0, 1/n)$ .

We will parametrize the dimensions by the number of columns  $n$ , and let the number of rows  $p = p_n$  grow with  $n$ . Specifically, we will assume that the limit

$$\gamma = \lim_{n \rightarrow \infty} \frac{p_n}{n} \quad (2)$$

is well-defined and finite.

Throughout the paper, we will fix sequences of symmetric  $p$ -by- $p$  matrices  $\Omega = \Omega_p$  and symmetric  $n$ -by- $n$  matrices  $\Pi = \Pi_n$  (dropping the dimension-specific subscripts). In Section 1.3, we will define loss functions defined in terms of these matrices. In order to have a well-defined asymptotic theory, we will need to assume that certain quantities have definite limits. We define:

$$\mu = \lim_{p \rightarrow \infty} \frac{1}{p} \text{tr}(\Omega^2) \quad (3)$$

and

$$\nu = \lim_{n \rightarrow \infty} \frac{1}{n} \text{tr}(\Pi^2). \quad (4)$$

For each  $k = 1, \dots, r$ , we also define

$$\alpha_k = \lim_{p \rightarrow \infty} \|\Omega \mathbf{u}_k\|^2 \quad (5)$$

and

$$\beta_k = \lim_{n \rightarrow \infty} \|\Pi \mathbf{v}_k\|^2. \quad (6)$$

## 1.2 Spectral denoisers

In Section 4, we will consider the class of denoisers of  $\mathbf{X}$  that modify the singular values of  $\mathbf{Y}$ , while leaving the singular vectors fixed. More precisely, we let

$$\mathbf{Y} = \sum_{i=1}^{\min(n,p)} \lambda_i \hat{\mathbf{u}}_i \hat{\mathbf{v}}_i^T \quad (7)$$

be the singular value decomposition of  $\mathbf{Y}$ . We then want to find the optimal values  $\hat{t}_1, \dots, \hat{t}_r$  so that

$$\hat{\mathbf{X}} = \sum_{k=1}^r \hat{t}_k \hat{\mathbf{u}}_k \hat{\mathbf{v}}_k^T \quad (8)$$

minimizes a specified loss function. We will describe the loss functions we use in this paper in Section 1.3.

Optimal denoisers of this form have been derived. For Frobenius loss, the optimal singular value shrinker is derived in [50]. A large family of orthogonally-invariant, block-decomposable loss functions are considered in [19]. Optimal singular value shrinkage for non-white noise matrices are derived in [45].

In Section 5, we will consider a generalization of this class of estimators, which we call a *localized matrix denoiser*. Briefly, a localized matrix denoiser changes the spectrum to optimally fit submatrices of  $\mathbf{X}$ , and then combines these submatrices to denoise all of  $\mathbf{X}$ . Each submatrix is denoised by choosing a particular loss function that selects its coordinates, and ignores the rest of the matrix. As we will show, localized denoising is always at least as good as the optimal spectral shrinker, but can be significantly better when  $\mathbf{X}$  exhibits *heterogeneity*, which we will formally define in Section 1.4.

### 1.3 The choice of loss function

In the high-dimensional regime, where  $p$  grows proportionally to  $n$ , the optimal choice of singular value shrinker depends crucially on the choice of loss function. Up until now, the only loss functions that have been considered are orthogonally-invariant. In the case of an isotropic Gaussian noise matrix (as we consider here), the paper [19] derives optimal shrinkers for loss-functions that are orthogonally-invariant and block-decomposable, meaning that if both  $\widehat{\mathbf{X}}$  and  $\mathbf{X}$  have the same block-diagonal structure, then the loss can be written as functions of the losses between the individual blocks.

In this work, we will consider a broader range of loss functions for shrinkage than have been previously considered. For the bulk of this paper, we will estimate the low-rank signal matrix  $\mathbf{X}$  with respect to the *weighted Frobenius loss*. For the symmetric weight matrices  $\Omega \in \mathbb{R}^{p \times p}$  and  $\Pi \in \mathbb{R}^{n \times n}$  from Section 1.1, define

$$\mathcal{L}_\omega(\widehat{\mathbf{X}}, \mathbf{X}) = \|\Omega(\widehat{\mathbf{X}} - \mathbf{X})\Pi\|_F^2, \quad (9)$$

where  $\|\cdot\|_F$  denotes the matrix Frobenius norm. This type of loss function is used when the user pays different prices for errors in different rows and columns.

We will study estimators  $\widehat{\mathbf{X}}$  of  $\mathbf{X}$  that minimize the asymptotic weighted mean squared error:

$$\text{AMSE}_\omega = \lim_{n \rightarrow \infty} \|\Omega(\widehat{\mathbf{X}} - \mathbf{X})\Pi\|_F^2. \quad (10)$$

It will follow from our analysis that this asymptotic loss is well-defined.

In Section 4.3, we will consider an even broader class of weighted loss functions, derived by introducing weights into the loss functions considered in [19]. More specifically, these will be loss functions of the form

$$\mathcal{L}_\omega(\widehat{\mathbf{X}}, \mathbf{X}) = \mathcal{L}(\Omega\widehat{\mathbf{X}}\Pi, \Omega\mathbf{X}\Pi), \quad (11)$$

where  $\mathcal{L}$  is an orthogonally-invariant, block-decomposable loss function. This extension requires us to impose an additional, albeit very weak, modeling assumption on the signal components.

We briefly note that weighted loss functions of the kind we study here have been employed in a variety of statistical applications, beyond the matrix denoising problem we are analyzing. For example, “utility-based regression” is concerned with non-uniform costs in the target variables [54]. Weighted quadratic loss functions are used in actuarial applications [12] and economic risk assessment [34]. Other kinds of weights used in a linear regression setting include, for example, weighting observations by propensity scores [16]. The Procrustes problem [21] has also been studied with the use of the type of weighted loss functions we consider here [43, 37]. Computational methods for matrix approximations with weighted loss functions have been considered as well [40, 52].

### 1.4 Heterogeneity, genericity, and weighted orthogonality

One of the aspects of the theory of matrix denoising we will explore is the role of the distribution of the signal matrix  $\mathbf{X}$ ’s singular vectors,  $\mathbf{u}_1, \dots, \mathbf{u}_r$  and  $\mathbf{v}_1, \dots, \mathbf{v}_r$ . We will say that a unit vector  $\mathbf{x} \in \mathbb{R}^m$  is “generic” with respect to an  $m$ -by- $m$  positive-semidefinite matrix  $\mathbf{A}$  if it satisfies

$$\mathbf{x}^T \mathbf{A} \mathbf{x} \sim \frac{1}{m} \text{tr}(\mathbf{A}), \quad (12)$$

where “ $\sim$ ” indicates that the difference between the two sides vanishes almost surely as  $m \rightarrow \infty$ . By contrast, we say that  $\mathbf{x}$  is “heterogeneous” if it is not generic. Informally, this means that the energy of the vectors is not uniformly distributed across its coordinates in the eigenbasis of  $\mathbf{A}$ . Indeed, if  $\mathbf{A} = \sum_{k=1}^m h_k \mathbf{w}_k \mathbf{w}_k^T$  is the eigendecomposition of  $\mathbf{A}$ , then

$$\mathbf{x}^T \mathbf{A} \mathbf{x} = \sum_{k=1}^m h_k \langle \mathbf{x}, \mathbf{w}_k \rangle^2. \quad (13)$$

If the energy of  $\mathbf{x}$  is equally spread out across the  $\mathbf{w}_k$ , then  $\langle \mathbf{x}, \mathbf{w}_k \rangle \sim 1/\sqrt{m}$ , and so  $\mathbf{x}^T \mathbf{A} \mathbf{x} \sim \text{tr}(\mathbf{A})/m$ . Note too that from the Hanson-Wright inequality [24, 57, 48], random unit vectors  $\mathbf{x}$  from suitably regular distributions will be generic.

Given a collection of vectors  $\mathbf{x}_1, \dots, \mathbf{x}_k \in \mathbb{R}^m$ , we will say that they satisfy the *weighted orthogonality condition* with respect to a positive-semidefinite matrix  $\mathbf{A}$  if

$$\mathbf{x}_i^T \mathbf{A} \mathbf{x}_j \sim 0 \quad (14)$$

whenever  $i \neq j$ . In other words, the  $\mathbf{x}_j$  are asymptotically orthogonal with respect to the weighted inner product defined by  $\mathbf{A}$ . Note that this condition will hold if the  $\mathbf{x}_j$  are independent random unit vectors from a suitable distribution (see [5]).

## 1.5 Relation to previous work and our contributions

This paper is concerned with spectral methods for estimation with respect to weighted loss functions, such as weighted quadratic loss. In previous work, optimal shrinkers have been derived for unweighted Frobenius loss [50, 45], as well as other orthogonally-invariant and block-decomposable loss functions [19]. However, adapting this method to weighted loss functions requires a more refined analysis of the asymptotic properties of the spiked model, which we develop here.

When the noise matrix is isotropic and the loss function is orthogonally-invariant, singular value shrinkage is known to be optimal in the absence of any prior information on the signal matrix  $\mathbf{X}$ . More precisely, in [50] it is shown that when using orthogonally-invariant loss functions, singular value shrinkage is optimal in the average case, meaning when  $\mathbf{X}$ ’s singular vectors are drawn from a uniform prior over the sphere. In the same spirit, in [17] it is shown that singular value shrinkage is optimal (using orthogonally-invariant loss functions) in the minimax sense. That is, its worst-case loss over all signal matrices  $\mathbf{X}$  is no greater than the worst-case loss of any other procedure.

The local denoisers we introduce in this paper are always at least as good as singular value shrinkage, and so inherit the aforementioned optimality properties. However, our new method is strictly better than shrinkage when the signal matrix’s singular vectors are heterogeneous, in the sense defined in Section 1.4.

In Section 2, we will discuss two motivating examples for spectral denoising with weighted loss functions. These examples arise even when the original problem objective is an unweighted estimation of  $\mathbf{X}$ . Specifically, in Section 2.1 we discuss heteroscedastic noise matrices, and in Section 2.2 we discuss missing data problems. The example of optimal denoising with heteroscedastic noise is considered in more depth in our paper [41]. The problem of spectral denoising for missing data problems — and more generally, the *linearly transformed spiked model* — is studied in [14]; however, our new method is optimal for unweighted estimation of  $\mathbf{X}$ , whereas the method of [14] is optimal only for a particular choice of weighted loss function.

In Section 3, we will derive new asymptotic results on the spiked model. These extend results we derived previously in [41]; in particular, the use of arbitrary weight functions and the derivation of the cosines between cross-terms is new. In Section 4.1 and use these asymptotics to derive optimal spectral estimators for weighted Frobenius loss. In Section 4.2, we will show that under weighted orthogonality, there are closed formulas for these shrinkers. In Section 4.3, we show that under weighted orthogonality, we can also derive optimal spectral estimators for weighted versions of the loss functions considered in [19].

In Section 5, we will use these optimal spectral estimators to derive the method localized denoising, which exploits heterogeneity of the signal matrix’s singular vectors in the estimation procedure. The unweighted AMSE of localized shrinkage is never worse than that of shrinkage, and can be significantly better if the signal is heterogeneous. In Section 5.2 we identify regimes in which our modified method is strictly better than singular value shrinkage. In Section 5.3, we compare our new method for denoising a submatrix  $\mathbf{X}_0$  of  $\mathbf{X}$

to performing singular value shrinkage on the submatrix. We illustrate our theoretical results via numerical simulations in Section 6.

## 2 Two motivating examples

In this section, we will describe two examples where we wish to estimate a target matrix  $\mathbf{X}$  with respect to ordinary, unweighted Frobenius loss, but other aspects of the statistical model lead us to perform singular value denoising with respect to a weighted loss function. That is, even when our ultimate goal is unweighted estimation of  $\mathbf{X}$ , a natural intermediate step of the estimation procedure requires the use of a weighted loss function. One-sided versions of the models we discuss here appear in [41] and [14].

### 2.1 Doubly-heteroscedastic noise

Suppose we observe a matrix  $\mathbf{Y} = \mathbf{X} + \mathbf{N}$ , where  $\mathbf{N}$  is a heteroscedastic noise matrix of the form

$$\mathbf{N} = \mathbf{A}^{1/2} \mathbf{G} \mathbf{B}^{1/2}, \quad (15)$$

where  $\mathbf{G}$  has iid entries with distribution  $N(0, 1/n)$ , and  $\mathbf{A} \in \mathbb{R}^{p \times p}$  and  $\mathbf{B} \in \mathbb{R}^{n \times n}$  are diagonal matrices with positive diagonal entries. Such an observation matrix arises in the setting where we observe independently-drawn vectors of the form  $\mathbf{y}_j = \mathbf{x}_j + b_j^{1/2} \varepsilon_j$ , where

$$\mathbf{x}_j = \sum_{k=1}^r \ell_k^{1/2} z_{jk} \mathbf{u}_k \quad (16)$$

where  $\varepsilon_i \sim N(\mathbf{0}, \mathbf{A})$ , and the  $z_{jk}$  are independent random variables. Each observation has heteroscedastic noise, and also a different total noise level. In the case where  $b_j = 1$  for all  $j$ , i.e.  $\mathbf{B} = \mathbf{I}_n$ , this is the model considered in [58] and [41]; here, we extend the model to permit each observation to have differing overall noise strength, which is also an extension of the model in [25, 26, 27]. Random matrices with a rank 1 variance structure have also been studied in [22, 23].

Setting  $\mathbf{v}_k = (z_{1k}, \dots, z_{nk})^T / \sqrt{n}$ , we can write:

$$\mathbf{X} = \sum_{k=1}^r \ell_k^{1/2} \mathbf{u}_k \mathbf{v}_k^T. \quad (17)$$

One may use the method of [45] to perform singular value shrinkage on  $\mathbf{Y} = \mathbf{X} + \mathbf{N}$  to estimate  $\mathbf{X}$ . However, we will show in Section 2.1.1 that if the singular vectors are generic with respect to  $\mathbf{A}^{-1/2}$  and  $\mathbf{B}^{-1/2}$ , then the signal strength increases relative to the noise if we perform a *whitening* transformation on the data, replacing  $\mathbf{Y}$  by  $\tilde{\mathbf{Y}}$  defined by

$$\tilde{\mathbf{Y}} = \mathbf{A}^{-1/2} \mathbf{Y} \mathbf{B}^{-1/2}. \quad (18)$$

We now have  $\tilde{\mathbf{Y}} = \tilde{\mathbf{X}} + \mathbf{G}$ , where  $\tilde{\mathbf{X}} = \mathbf{A}^{-1/2} \mathbf{X} \mathbf{B}^{-1/2}$  and  $\mathbf{G}$  has iid  $N(0, 1/n)$  entries. The matrix  $\tilde{\mathbf{X}}$  can be written as:

$$\tilde{\mathbf{X}} = \sum_{k=1}^r \ell_k^{1/2} (\mathbf{A}^{-1/2} \mathbf{u}_k) (\mathbf{B}^{-1/2} \mathbf{v}_k)^T = \sum_{k=1}^r \tilde{\ell}_k^{1/2} \tilde{\mathbf{u}}_k \tilde{\mathbf{v}}_k^T, \quad (19)$$

where  $\tilde{\ell}_k = \ell_k \|\mathbf{A}^{-1/2} \mathbf{u}_k\|^2 \|\mathbf{B}^{-1/2} \mathbf{v}_k\|^2$ ,  $\tilde{\mathbf{u}}_k = \mathbf{A}^{-1/2} \mathbf{u}_k / \|\mathbf{A}^{-1/2} \mathbf{u}_k\|$ , and  $\tilde{\mathbf{v}}_k = \mathbf{B}^{-1/2} \mathbf{v}_k / \|\mathbf{B}^{-1/2} \mathbf{v}_k\|$ .

We now apply a singular value denoiser to  $\tilde{\mathbf{Y}}$ , and then unwhiten the resulting estimator  $f(\tilde{\mathbf{Y}})$  to obtain the estimate  $\hat{\mathbf{X}} = \mathbf{A}^{1/2} f(\tilde{\mathbf{Y}}) \mathbf{B}^{1/2}$  of  $\mathbf{X}$ . How should the function  $f$  (which transforms only the singular values, not the singular vectors, of the input matrix) be chosen? The loss can be written as follows:

$$\|\hat{\mathbf{X}} - \mathbf{X}\|_F^2 = \|\mathbf{A}^{1/2} f(\tilde{\mathbf{Y}}) \mathbf{B}^{1/2} - \mathbf{A}^{1/2} \tilde{\mathbf{X}} \mathbf{B}^{1/2}\|_F^2 = \|\mathbf{A}^{1/2} (f(\tilde{\mathbf{Y}}) - \tilde{\mathbf{X}}) \mathbf{B}^{1/2}\|_F^2, \quad (20)$$

which is a weighted loss between  $f(\tilde{\mathbf{Y}})$  and  $\tilde{\mathbf{X}}$ . Consequently, the spectral estimator  $f(\tilde{\mathbf{Y}})$  should be chosen to minimize this weighted Frobenius loss. That is, if our goal is to estimate  $\mathbf{X}$  in Frobenius loss, then the singular value denoiser we apply to  $\tilde{\mathbf{Y}}$  should not minimize the Frobenius loss with  $\tilde{\mathbf{X}}$ , but rather the weighted Frobenius loss, with weight matrices  $\mathbf{A}^{1/2}$  and  $\mathbf{B}^{1/2}$ .

### 2.1.1 Whitening maximizes the SNR for generic signal matrices

We show that the whitening transformation increases certain measures of the matrix's signal-to-noise ratio. We will assume throughout this section that the  $\mathbf{u}_k$  (respectively,  $\mathbf{v}_k$ ) are generic with respect to  $\mathbf{A}$  (respectively,  $\mathbf{B}$ ), and that they satisfy the pairwise orthogonality condition with respect to  $\mathbf{A}$  (respectively  $\mathbf{B}$ ). Following [41], we define the operator norm signal-to-noise ratio (SNR) for each component of the signal matrix  $\mathbf{X}$  by:

$$\text{SNR}_{\text{op}}^{(k)} = \frac{\ell_k}{\|\mathbf{N}\|_{\text{op}}^2}, \quad (21)$$

which is the asymptotic ratio of the squared operator norm of each component  $\ell_k^{1/2} \mathbf{u}_k \mathbf{v}_k^\top$  of  $\mathbf{X}$  and the squared operator norm of the noise. After whitening the noise matrix, the observation changes into  $\tilde{\mathbf{Y}} = \tilde{\mathbf{X}} + \mathbf{G}$ , where  $\tilde{\mathbf{X}}$  is still rank  $r$ , and in 1-1 correspondence with  $\mathbf{X}$ . Consequently, the operator norm SNR after whitening is:

$$\widetilde{\text{SNR}}_{\text{op}}^{(k)} = \frac{\tilde{\ell}_k}{\|\mathbf{G}\|_{\text{op}}^2}. \quad (22)$$

Note that because  $\mathbf{u}_k$  and  $\mathbf{v}_k$  are generic and weighted-orthogonal, the vectors  $\tilde{\mathbf{u}}_k$  (respectively,  $\tilde{\mathbf{v}}_k$ ) are asymptotically pairwise orthogonal, and

$$\tilde{\ell}_k \sim \ell_k \cdot \frac{\text{tr}(\mathbf{A}^{-1})}{p} \cdot \frac{\text{tr}(\mathbf{B}^{-1})}{n}. \quad (23)$$

Another way of measuring the SNR is to take the ratio of the squared Frobenius norms. Each component of the original observation matrix  $\mathbf{Y} = \mathbf{X} + \mathbf{N}$  has SNR equal to:

$$\text{SNR}_{\text{F}}^{(k)} = \frac{\ell_k}{\|\mathbf{N}\|_{\text{F}}^2}. \quad (24)$$

After whitening the noise, each component of the resulting matrix  $\tilde{\mathbf{Y}} = \tilde{\mathbf{X}} + \mathbf{G}$  has SNR equal to:

$$\widetilde{\text{SNR}}_{\text{F}}^{(k)} = \frac{\tilde{\ell}_k}{\|\mathbf{G}\|_{\text{F}}^2}. \quad (25)$$

We will prove the following result, which is a simple extension of those found in [41] and [44] to the setting of weighted rows and columns:

**Proposition 2.1.** *Suppose  $\mathbf{A}$  and  $\mathbf{B}$  are not both equal to constant multiples of the identity. Then in the limit  $p/n \rightarrow \gamma$ ,*

$$\frac{\widetilde{\text{SNR}}_{\text{op}}^{(k)}}{\text{SNR}_{\text{op}}^{(k)}} > 1, \quad (26)$$

and

$$\frac{\widetilde{\text{SNR}}_{\text{F}}^{(k)}}{\text{SNR}_{\text{F}}^{(k)}} > 1. \quad (27)$$

In other words, if the signal is generic, then the SNR increases after whitening the noise; energy is transferred from the noise component to the signal component. Additional benefits of noise whitening are considered in detail in [41].

The proof of Proposition 2.1 is a straightforward extension of the analogous results from [41] and [44]. We provide a proof for completeness.

*Proof of Proposition 2.1.* To prove (26), we begin by deriving a lower bound on the operator norm of the noise matrix  $\mathbf{N} = \mathbf{A}^{1/2}\mathbf{G}\mathbf{B}^{1/2}$ . We let  $\mathbf{a}$  and  $\mathbf{b}$  be unit vectors so that  $\mathbf{G}^\top \mathbf{b} = \|\mathbf{G}\|_{\text{op}} \mathbf{a}$ . Then

$$\|\mathbf{G}\mathbf{B}^{1/2}\|_{\text{op}} \geq \|\mathbf{B}^{1/2}\mathbf{G}^\top \mathbf{b}\| = \|\mathbf{G}\|_{\text{op}} \|\mathbf{B}^{1/2}\mathbf{a}\|. \quad (28)$$

Next, we take unit vectors  $\mathbf{c}$  and  $\mathbf{d}$  so that  $\mathbf{G}\mathbf{B}^{1/2}\mathbf{d} = \|\mathbf{G}\mathbf{B}^{1/2}\|_{\text{op}} \mathbf{c}$ . Then we have

$$\|\mathbf{N}\|_{\text{op}}^2 \geq \|\mathbf{A}^{1/2}\mathbf{G}\mathbf{B}^{1/2}\mathbf{d}\|^2 = \|\mathbf{G}\mathbf{B}^{1/2}\|_{\text{op}}^2 \|\mathbf{A}^{1/2}\mathbf{c}\|^2 \geq \|\mathbf{G}\|_{\text{op}} \cdot \|\mathbf{B}^{1/2}\mathbf{a}\|^2 \cdot \|\mathbf{A}^{1/2}\mathbf{c}\|^2. \quad (29)$$

Since the distribution of  $\mathbf{G}$  is orthogonally invariant, the distributions of  $\mathbf{a}$  and  $\mathbf{c}$  are uniform over the unit spheres in  $\mathbb{R}^p$  and  $\mathbb{R}^n$ , respectively. Consequently,  $\|\mathbf{B}^{1/2}\mathbf{a}\|^2 \sim \text{tr}(\mathbf{B})/n$  and  $\|\mathbf{A}^{1/2}\mathbf{c}\|^2 \sim \text{tr}(\mathbf{A})/p$ . Therefore,

$$\|\mathbf{N}\|_{\text{op}}^2 \geq (\text{tr}(\mathbf{A})/p) \cdot (\text{tr}(\mathbf{B})/n) \cdot \|\mathbf{G}\|_{\text{op}}^2 \sim (\text{tr}(\mathbf{A})/p) \cdot (\text{tr}(\mathbf{B})/n) \cdot (1 + \sqrt{\gamma})^2, \quad (30)$$

where the inequality holds almost surely in the large  $p$ , large  $n$  limit. We have used that the spectral norm of  $\mathbf{G}$  converges almost surely to  $1 + \sqrt{\gamma}$ ; see, e.g., [3].

Now we can show the improvement in operator norm SNR. We have:

$$\begin{aligned} \text{SNR}_{\text{op}}^{(k)} &= \frac{\ell_k}{\|\mathbf{N}\|_{\text{op}}^2} \lesssim \frac{\ell_k}{(\text{tr}(\mathbf{A})/p) \cdot (\text{tr}(\mathbf{B})/n) \cdot (1 + \sqrt{\gamma})^2} \\ &< \frac{\ell_k \cdot (\text{tr}(\mathbf{A}^{-1})/p) \cdot (\text{tr}(\mathbf{B}^{-1})/n)}{(1 + \sqrt{\gamma})^2} = \frac{\tilde{\ell}_k}{\|\mathbf{G}\|_{\text{op}}^2} = \widetilde{\text{SNR}}_{\text{op}}^{(k)}, \end{aligned} \quad (31)$$

where we have used Jensen's inequality for the strict inequality. This completes the proof of (26).

To prove (27), we first observe that

$$\frac{1}{p} \|\mathbf{N}\|_{\text{F}}^2 \sim \frac{\text{tr}(\mathbf{A})}{p} \cdot \frac{\text{tr}(\mathbf{B})}{n}. \quad (32)$$

Indeed, if we let  $F_i = \sum_{k=1}^n b_j G_{ij}^2$ , then standard concentration results (see, e.g., [56]) show that  $\max_i |F_i - \text{tr}(\mathbf{B})/n| \rightarrow 0$  almost surely; it then follows that:

$$\frac{1}{p} \|\mathbf{N}\|_{\text{F}}^2 = \frac{1}{p} \sum_{i=1}^p a_i F_i = \frac{\text{tr}(\mathbf{B})}{n} \cdot \frac{1}{p} \sum_{i=1}^p a_i + \frac{1}{p} \sum_{i=1}^p a_i (F_i - \text{tr}(\mathbf{B})/n) \sim \frac{\text{tr}(\mathbf{A})}{p} \cdot \frac{\text{tr}(\mathbf{B})}{n}. \quad (33)$$

Since  $\|\mathbf{G}\|_{\text{F}}^2/p \sim 1$ , we have

$$\frac{\widetilde{\text{SNR}}_{\text{F}}^{(k)}}{\text{SNR}_{\text{F}}^{(k)}} = \ell_k \cdot (\text{tr}(\mathbf{A}^{-1})/p) \cdot (\text{tr}(\mathbf{B}^{-1})/n) \cdot \frac{(\text{tr}(\mathbf{A})/p) \cdot (\text{tr}(\mathbf{B})/n)}{\ell_k} > 1, \quad (34)$$

where we have once again used Jensen's inequality. This proves (27).  $\square$

## 2.2 Matrices with missing/unobserved values

We consider the setting where  $\mathbf{X}$  is a low-rank target matrix we wish to recover, but rather than observe  $\mathbf{X} + \mathbf{G}$ , we observe only some subset of the entries. The problem of estimating a matrix from a subset of its entries is known as *matrix completion*; it has been extensively studied, in both the noise-free and high-noise regimes [35, 32, 9, 47, 33, 36, 28, 10, 14].

In this section, we will adopt a heterogeneous, rank 1 sampling model, which is considered in [11]. Specifically, we suppose that the rows and columns are sampled independently, with row  $i$  sampled with probability  $q_i^r$ , and column  $j$  sampled with probability  $q_j^c$ ; that is, entry  $(i, j)$  of  $\mathbf{X} + \mathbf{G}$  is sampled with probability  $q_i^r q_j^c$ . We observe  $\mathcal{F}(\mathbf{X} + \mathbf{G})$ , where  $\mathcal{F} : \mathbb{R}^{p \times n} \rightarrow \mathbb{R}^M$  is the subsampling operator, with  $M$  being the number of sampled entries.

Following the approach from [14], we consider the backprojected matrix  $\mathbf{Y} = \mathcal{F}^*(\mathcal{F}(\mathbf{X} + \mathbf{G})) \in \mathbb{R}^{p \times n}$ , in which the unobserved entries are replaced by 0's. We write  $\mathbf{Y} = \mathcal{F}^*(\mathcal{F}(\mathbf{X})) + \mathcal{F}^*(\mathcal{F}(\mathbf{G}))$ . We can show that asymptotically,  $\mathcal{F}^*(\mathcal{F}(\mathbf{X}))$  behaves like the matrix  $\mathbf{P}\mathbf{X}\mathbf{Q}$ . More precisely, we have the following result:

**Proposition 2.2.** Suppose  $\max_{1 \leq k \leq r} \|\mathbf{u}_k\|_\infty \|\mathbf{v}_k\|_\infty = o(n^{-1/2})$ . Then in the limit  $p/n \rightarrow \gamma$ ,

$$\|\mathcal{F}^*(\mathcal{F}(\mathbf{X})) - \mathbf{P}\mathbf{X}\mathbf{Q}\|_{op} \rightarrow 0 \quad (35)$$

almost surely.

The proof of Proposition 2.2 is a straightforward generalization of the analogous one-sided result in [14]. We include it here for completeness.

*Proof of Proposition 2.2.* Let  $\delta_{ij}$  be 1 if entry  $(i, j)$  is sampled, and 0 otherwise. Then  $\delta_{ij} \sim \text{Bernoulli}(p_j q_j)$ . Let  $\Delta = (\delta_{ij})_{i,j}$ ; then  $\mathcal{F}^*(\mathcal{F}(\mathbf{X})) = \Delta \odot \mathbf{X}$ , where  $\odot$  denotes the Hadamard product. Let  $\mathbf{q}_r = (q_1^r, \dots, q_p^r)^T$  and  $\mathbf{q}_c = (q_1^c, \dots, q_n^c)^T$ . The matrix  $\Delta - \mathbf{q}_r \mathbf{q}_c^T$  is a random matrix with mean zero, whose entries are uniformly bounded. It follows from Corollary 2.3.5 of [53] that  $\|\Delta - \mathbf{q}_r \mathbf{q}_c^T\|_{op}/\sqrt{n} \leq A$  a.s. as  $n \rightarrow \infty$ , for some constant  $A > 0$ .

Now  $\mathbf{P}\mathbf{X}\mathbf{Q} = \mathbf{X} \odot (\mathbf{q}_r \mathbf{q}_c^T)$ . Consequently,  $\Delta \odot \mathbf{X} - \mathbf{P}\mathbf{X}\mathbf{Q} = (\Delta - \mathbf{q}_r \mathbf{q}_c^T) \odot \mathbf{X}$ . Since  $\mathbf{X} = \sum_{k=1}^r t_k \mathbf{u}_k \mathbf{v}_k^T$ , it is enough to show that

$$\|(\Delta - \mathbf{q}_r \mathbf{q}_c^T) \odot \mathbf{u}_k \mathbf{v}_k^T\|_{op} \rightarrow 0 \quad (36)$$

almost surely, for each  $k$ .

Suppose  $\mathbf{a}$  and  $\mathbf{b}$  are two unit vectors. Then

$$|\mathbf{a}^T [(\Delta - \mathbf{q}_r \mathbf{q}_c^T) \odot \mathbf{u}_k \mathbf{v}_k^T] \mathbf{b}| = |(\mathbf{a} \odot \mathbf{u}_k)^T (\Delta - \mathbf{q}_r \mathbf{q}_c^T) (\mathbf{b} \odot \mathbf{v}_k)| \leq A \sqrt{n} \|\mathbf{a} \odot \mathbf{u}_k\| \|\mathbf{b} \odot \mathbf{v}_k\| \quad (37)$$

almost surely as  $n \rightarrow \infty$ .

Now, since  $\mathbf{a}$  is a unit vector,

$$\|\mathbf{a} \odot \mathbf{u}_k\| = \sqrt{\sum_{j=1}^p a_j^2 u_{jk}^2} \leq \|\mathbf{u}_k\|_\infty \quad (38)$$

and similarly,

$$\|\mathbf{b} \odot \mathbf{v}_k\| \leq \|\mathbf{v}_k\|_\infty. \quad (39)$$

Since  $\max_{1 \leq k \leq r} \|\mathbf{u}_k\|_\infty \|\mathbf{v}_k\|_\infty = o(n^{-1/2})$ , the result follows.  $\square$

Now, let  $\mathbf{N} = \mathcal{F}^*(\mathcal{F}(\mathbf{G}))$ . Then  $N_{ij} = \delta_{ij} G_{ij}$ , where  $\delta_{ij}$  is 1 if entry  $(i, j)$  is sampled, and 0 otherwise. Then  $N_{ij}$  has variance  $q_i^r q_j^c$ . Consequently, we can whiten the noise matrix by applying  $\mathbf{P}^{-1/2}$  and  $\mathbf{Q}^{-1/2}$ ; Proposition 2.1 suggests this will improve estimation of the matrix. To that end, we define

$$\tilde{\mathbf{Y}} = \mathbf{P}^{-1/2} \mathbf{Y} \mathbf{Q}^{-1/2} = \tilde{\mathbf{X}} + \tilde{\mathbf{G}}, \quad (40)$$

where  $\tilde{\mathbf{X}} = \mathbf{P}^{-1/2} \mathcal{F}^*(\mathcal{F}(\mathbf{X})) \mathbf{Q}^{-1/2}$ , and  $\tilde{\mathbf{G}} = \mathbf{P}^{-1/2} \mathbf{N} \mathbf{Q}^{-1/2}$ . Then  $\tilde{\mathbf{G}}$  is a random matrix where each entry has mean zero and variance 1.

From Proposition 2.2, asymptotically the matrix  $\tilde{\mathbf{X}}$  behaves like  $\mathbf{P}^{1/2} \mathbf{X} \mathbf{Q}^{1/2}$ . Consequently, if we perform singular value denoising to  $\tilde{\mathbf{Y}}$ , we will be producing an estimate of  $\mathbf{P}^{1/2} \mathbf{X} \mathbf{Q}^{1/2}$ , not  $\mathbf{X}$  itself. Therefore, to estimate  $\mathbf{X}$  we should perform denoising to  $\tilde{\mathbf{Y}}$  with respect to the weighted loss function

$$\mathcal{L}(\hat{\mathbf{X}}, \mathbf{X}) = \|\mathbf{P}^{-1/2} (\hat{\mathbf{X}} - \mathbf{X}) \mathbf{Q}^{-1/2}\|_F^2. \quad (41)$$

We then apply  $\mathbf{P}^{-1/2}$  and  $\mathbf{Q}^{-1/2}$  to the resulting matrix, to obtain an estimator of  $\mathbf{X}$  itself.

### 3 Mathematical theory for the spiked model

In this section, we establish the necessary mathematical ingredients to derive the optimal singular value denoisers for weighted loss functions. In Sections 3.1 and 3.2, we derive new asymptotic formulas for the angles between the singular vectors of population matrices and observed matrices. In Section 3.3, we formulate and solve a general optimization problem over the singular values of a matrix.

### 3.1 Asymptotic results

In this section, we derive the asymptotic limits of the angles between certain vectors. First, we recall that  $t_1 > \dots > t_r > 0$  are the singular values of the matrix  $\mathbf{X}$ , and  $\mathbf{u}_1, \dots, \mathbf{u}_r$  and  $\mathbf{v}_1, \dots, \mathbf{v}_r$  the corresponding left and right singular vectors. We denote by  $\lambda_1 > \dots > \lambda_r > 0$  the  $r$  largest singular values of the noisy matrix  $\mathbf{Y} = \mathbf{X} + \mathbf{G}$ , and  $\hat{\mathbf{u}}_1, \dots, \hat{\mathbf{u}}_r$  and  $\hat{\mathbf{v}}_1, \dots, \hat{\mathbf{v}}_r$  the corresponding left and right singular vectors. We also recall that  $\alpha_k = \|\Omega \mathbf{u}_k\|^2$  and  $\beta_k = \|\Pi \mathbf{v}_k\|^2$ .

Now we define

$$\mathbf{u}_k^\omega = \frac{\Omega \mathbf{u}_k}{\|\Omega \mathbf{u}_k\|}, \quad \hat{\mathbf{u}}_k^\omega = \frac{\Omega \hat{\mathbf{u}}_k}{\|\Omega \hat{\mathbf{u}}_k\|}, \quad \mathbf{v}_k^\omega = \frac{\Pi \mathbf{v}_k}{\|\Pi \mathbf{v}_k\|}, \quad \hat{\mathbf{v}}_k^\omega = \frac{\Pi \hat{\mathbf{v}}_k}{\|\Pi \hat{\mathbf{v}}_k\|}. \quad (42)$$

We will refer to the vectors  $\mathbf{u}_k$ ,  $\mathbf{u}_k^\omega$ ,  $\mathbf{v}_k$  and  $\mathbf{v}_k^\omega$ , which are never directly observed, as *population vectors*; and  $\hat{\mathbf{u}}_k$ ,  $\hat{\mathbf{u}}_k^\omega$ ,  $\hat{\mathbf{v}}_k$  and  $\hat{\mathbf{v}}_k^\omega$  as *empirical vectors*, since we do observe them.

We then define the limiting cosines

$$c_{jk}^\omega = \lim_{n \rightarrow \infty} \langle \hat{\mathbf{u}}_j^\omega, \mathbf{u}_k^\omega \rangle, \quad \tilde{c}_{jk}^\omega = \lim_{n \rightarrow \infty} \langle \hat{\mathbf{v}}_j^\omega, \mathbf{v}_k^\omega \rangle, \quad c_{jk} = \lim_{n \rightarrow \infty} \langle \hat{\mathbf{u}}_j, \mathbf{u}_k \rangle, \quad \tilde{c}_{jk} = \lim_{n \rightarrow \infty} \langle \hat{\mathbf{v}}_j, \mathbf{v}_k \rangle, \quad (43)$$

between empirical and population vectors;

$$d_{jk} = \lim_{n \rightarrow \infty} \langle \hat{\mathbf{u}}_j^\omega, \hat{\mathbf{u}}_k^\omega \rangle, \quad \tilde{d}_{jk} = \lim_{n \rightarrow \infty} \langle \hat{\mathbf{v}}_j^\omega, \hat{\mathbf{v}}_k^\omega \rangle, \quad (44)$$

between empirical vectors; and

$$e_{jk} = \lim_{n \rightarrow \infty} \langle \mathbf{u}_j^\omega, \mathbf{u}_k^\omega \rangle, \quad \tilde{e}_{jk} = \lim_{n \rightarrow \infty} \langle \mathbf{v}_j^\omega, \mathbf{v}_k^\omega \rangle, \quad (45)$$

between population vectors. Observe that  $d_{jj} = \tilde{d}_{jj} = e_{jj} = \tilde{e}_{jj} = 1$ . We will let  $c_k^\omega = c_{kk}^\omega$  and  $\tilde{c}_k^\omega = \tilde{c}_{kk}^\omega$ , and  $c_k = c_{kk}$  and  $\tilde{c}_k = \tilde{c}_{kk}$ .

**Remark 1.** Before stating the formulas for these quantities, we observe that in all cases there is an ambiguity of their signs, since the signs of singular vectors may be chosen arbitrarily. However, when we employ the formulas in Section 4 to derive optimal singular value denoisers, we will only make use of the products of cosines between left and right singular vectors, e.g. terms of the form  $d_{jk} \tilde{d}_{jk}$ . These quantities are in fact well-defined, since, for example, if we flip the sign of the vector  $\hat{\mathbf{u}}_k$ , we must also flip the sign of its associated vector  $\hat{\mathbf{v}}_k$ .

The first result is well-known in the literature (see e.g. [46, 6]).

**Proposition 3.1.** For  $1 \leq j, k \leq r$ ,

$$\lambda_k^2 = \begin{cases} (t_k^2 + 1) \left(1 + \frac{\gamma}{t_k^2}\right) & \text{if } j = k \text{ and } t_k > \gamma^{1/4}, \\ (1 + \sqrt{\gamma})^2, & \text{if } j \neq k \text{ or } t_k \leq \gamma^{1/4}, \end{cases} \quad (46)$$

$$c_{jk}^2 = \begin{cases} \frac{1-\gamma/t_k^4}{1+\gamma/t_k^2}, & \text{if } j = k \text{ and } t_k > \gamma^{1/4}, \\ 0, & \text{if } j \neq k \text{ or } t_k \leq \gamma^{1/4}, \end{cases} \quad (47)$$

and

$$\tilde{c}_{jk}^2 = \begin{cases} \frac{1-\gamma/t_k^4}{1+1/t_k^2}, & \text{if } j = k \text{ and } t_k > \gamma^{1/4}, \\ 0, & \text{if } j \neq k \text{ or } t_k \leq \gamma^{1/4}. \end{cases} \quad (48)$$

We now provide asymptotic formulas for  $\|\Omega \hat{\mathbf{u}}_k\|^2$  and  $\|\Pi \hat{\mathbf{v}}_k\|^2$  that relate them to the parameters  $\alpha_k$  and  $\beta_k$ . Since  $\|\Omega \hat{\mathbf{u}}_k\|^2$  and  $\|\Pi \hat{\mathbf{v}}_k\|^2$  can be directly measured, this will allow us to estimate  $\alpha_k$  and  $\beta_k$ .

**Proposition 3.2.** For  $1 \leq k \leq r$ , if  $t_k > \gamma^{1/4}$  then the following limits hold almost surely:

$$\lim_{p \rightarrow \infty} \|\Omega \hat{\mathbf{u}}_k\|^2 = c_k^2 \alpha_k + s_k^2 \mu, \quad (49)$$

and

$$\lim_{n \rightarrow \infty} \|\Pi \hat{\mathbf{v}}_k\|^2 = \tilde{c}_k^2 \beta_k + \tilde{s}_k^2 \nu. \quad (50)$$

Next, we state formulas for the terms  $c_{jk}^\omega$  and  $\tilde{c}_{jk}^\omega$ , the cosines between population and empirical vectors after applying the weight transformations and renormalizing.

**Proposition 3.3.** For  $1 \leq j, k \leq r$ ,

$$c_{jk}^\omega = \begin{cases} e_{jk} \cdot \sqrt{\frac{c_j^2 \alpha_j}{c_j^2 \alpha_j + s_j^2 \mu}}, & \text{if } t_j > \gamma^{1/4}, \\ 0, & \text{if } t_j \leq \gamma^{1/4}, \end{cases} \quad (51)$$

and

$$\tilde{c}_{jk}^\omega = \begin{cases} \tilde{e}_{jk} \cdot \sqrt{\frac{\tilde{c}_j^2 \beta_j}{\tilde{c}_j^2 \beta_j + \tilde{s}_j^2 \nu}}, & \text{if } t_j > \gamma^{1/4}, \\ 0, & \text{if } t_j \leq \gamma^{1/4}. \end{cases} \quad (52)$$

Finally, we give formulas for the terms  $d_{jk}$  and  $\tilde{d}_{jk}$ , the cosines between empirical vectors after applying the weight transformations and renormalizing. Note that these quantities are directly estimable, since we have access to the empirical vectors. As we will see in Section 4, we will use Proposition 3.4 to derive estimates for  $e_{jk}$  and  $\tilde{e}_{jk}$ .

**Proposition 3.4.** For  $1 \leq j \neq k \leq r$ ,

$$d_{jk} = \begin{cases} e_{jk} \cdot \sqrt{\frac{c_j^2 \alpha_j}{c_j^2 \alpha_j + s_j^2 \mu} \cdot \frac{c_k^2 \alpha_k}{c_k^2 \alpha_k + s_k^2 \mu}}, & \text{if } \min\{t_j, t_k\} > \gamma^{1/4}, \\ 0, & \text{if } \min\{t_j, t_k\} \leq \gamma^{1/4}, \end{cases} \quad (53)$$

and

$$\tilde{d}_{jk} = \begin{cases} \tilde{e}_{jk} \cdot \sqrt{\frac{\tilde{c}_j^2 \beta_j}{\tilde{c}_j^2 \beta_j + \tilde{s}_j^2 \nu} \cdot \frac{\tilde{c}_k^2 \beta_k}{\tilde{c}_k^2 \beta_k + \tilde{s}_k^2 \nu}}, & \text{if } \min\{t_j, t_k\} > \gamma^{1/4}, \\ 0, & \text{if } \min\{t_j, t_k\} \leq \gamma^{1/4}. \end{cases} \quad (54)$$

### 3.2 Proof of Propositions 3.2, 3.3 and 3.4

The proofs of Propositions 3.2, 3.3 and 3.4 are similar to those in [41], in that they rest on the same decomposition of the empirical singular vectors  $\hat{\mathbf{u}}_k$  and  $\hat{\mathbf{v}}_k$  into the signal and residual components. If  $\mathbf{a}$  and  $\mathbf{b}$  are vectors of the same dimension, we will write  $\mathbf{a} \sim \mathbf{b}$  as a short-hand for  $\|\mathbf{a} - \mathbf{b}\| \rightarrow 0$  almost surely as  $p, n \rightarrow \infty$ . The statements are symmetric in the left and right singular vectors, so for compactness we will only prove them for the left ones. The proofs for the other side are identical.

Because the noise matrix  $\mathbf{G}$  has an isotropic distribution, we can write:

$$\hat{\mathbf{u}}_k \sim c_k \mathbf{u}_k + s_k \tilde{\mathbf{u}}_k, \quad (55)$$

where  $\tilde{\mathbf{u}}_k$  is a unit vector that is uniformly random over the sphere in the subspace orthogonal to  $\mathbf{u}_1, \dots, \mathbf{u}_r$  (see [46]). Because  $\tilde{\mathbf{u}}_k$  is uniformly random, it is asymptotically orthogonal to any independent unit vector  $\mathbf{w}$ ; that is,

$$\tilde{\mathbf{u}}_k^T \mathbf{w} \sim 0. \quad (56)$$

Furthermore,  $\tilde{\mathbf{u}}_k$  satisfies the normalized trace formula, namely if  $\mathbf{A}$  is any matrix with bounded operator norm, then

$$\tilde{\mathbf{u}}_k^T \mathbf{A} \tilde{\mathbf{u}}_k \sim \frac{1}{p} \text{tr}(\mathbf{A}). \quad (57)$$

We refer the reader to [5, 24, 57, 48] for details. We will use (56) and (57) repeatedly. Furthermore, when  $j \neq k$  it follows from Lemma 3.5 in [41] that

$$\tilde{\mathbf{u}}_j^T \mathbf{A} \tilde{\mathbf{u}}_k \sim 0. \quad (58)$$

Applying  $\Omega$  to each side of (55), we have:

$$\Omega \hat{\mathbf{u}}_k \sim c_k \Omega \mathbf{u}_k + s_k \Omega \tilde{\mathbf{u}}_k. \quad (59)$$

The proofs of Propositions 3.2, 3.3 and 3.4 will follow by manipulating the asymptotic equation (59) appropriately, in conjunction with (56), (57) and (58).

### 3.2.1 Proof of Proposition 3.2

Taking the squared norm of each side of (59), we obtain:

$$\|\Omega \hat{\mathbf{u}}_k\|^2 \sim c_k^2 \|\Omega \mathbf{u}_k\|^2 + s_k^2 \|\Omega \tilde{\mathbf{u}}_k\|^2 \sim c_k^2 \alpha_k + s_k^2 \mu. \quad (60)$$

The first asymptotic equivalence follows from (56), and the second from (57). This is the desired result.

### 3.2.2 Proof of Proposition 3.3

We take inner products of each side of (59) (replacing  $k$  with  $j$ ) with  $\Omega \mathbf{u}_j$ :

$$\langle \Omega \hat{\mathbf{u}}_j, \Omega \mathbf{u}_k \rangle \sim c_j \langle \Omega \mathbf{u}_j, \Omega \mathbf{u}_k \rangle + s_j \langle \Omega \tilde{\mathbf{u}}_j, \Omega \mathbf{u}_k \rangle \sim c_j \langle \Omega \mathbf{u}_j, \Omega \mathbf{u}_k \rangle \sim c_j e_{jk} \sqrt{\alpha_j \alpha_k}, \quad (61)$$

where we have used (56). From Proposition 3.2,

$$c_{jk}^\omega = \frac{\langle \Omega \hat{\mathbf{u}}_j, \Omega \mathbf{u}_k \rangle}{\|\Omega \hat{\mathbf{u}}_j\| \|\Omega \mathbf{u}_k\|} \sim \frac{c_j e_{jk} \sqrt{\alpha_j \alpha_k}}{\|\Omega \hat{\mathbf{u}}_j\| \|\Omega \mathbf{u}_k\|} \sim c_j e_{jk} \sqrt{\frac{\alpha_j}{c_j^2 \alpha_j + s_j^2 \mu}}, \quad (62)$$

which is the desired result.

### 3.2.3 Proof of Proposition 3.4

From (59), we have

$$\langle \Omega \hat{\mathbf{u}}_j, \Omega \hat{\mathbf{u}}_k \rangle \sim c_j c_k \langle \Omega \mathbf{u}_j, \Omega \mathbf{u}_k \rangle + s_j s_k \langle \Omega \tilde{\mathbf{u}}_j, \Omega \tilde{\mathbf{u}}_k \rangle + s_j c_k \langle \Omega \tilde{\mathbf{u}}_j, \Omega \mathbf{u}_k \rangle + c_j s_k \langle \Omega \mathbf{u}_j, \Omega \tilde{\mathbf{u}}_k \rangle. \quad (63)$$

From (56) and (58), the terms involving  $\tilde{\mathbf{u}}_j$  and  $\tilde{\mathbf{u}}_k$  vanish, and we are left with

$$\langle \Omega \hat{\mathbf{u}}_j, \Omega \hat{\mathbf{u}}_k \rangle \sim c_j c_k \langle \Omega \mathbf{u}_j, \Omega \mathbf{u}_k \rangle \sim c_j c_k e_{jk} \sqrt{\alpha_j \alpha_k}. \quad (64)$$

Consequently, from Proposition 3.2 we have:

$$d_{jk} = \frac{\langle \Omega \hat{\mathbf{u}}_j, \Omega \hat{\mathbf{u}}_k \rangle}{\|\Omega \hat{\mathbf{u}}_j\| \|\Omega \hat{\mathbf{u}}_k\|} \sim c_j c_k e_{jk} \sqrt{\frac{\alpha_j \alpha_k}{(c_j^2 \alpha_j + s_j^2 \mu)(c_k^2 \alpha_k + s_k^2 \mu)}}. \quad (65)$$

This completes the proof.

### 3.3 Minimizing Frobenius loss

We consider a general scenario, in which we have a target matrix of the form

$$\mathbf{A} = \sum_{k=1}^r t_k \mathbf{w}_k \mathbf{z}_k^T \quad (66)$$

where  $\mathbf{w}_k \in \mathbb{R}^p$ ,  $\mathbf{z}_k \in \mathbb{R}^n$  are unknown vectors, and  $t_1, \dots, t_r$  are known numbers. We suppose we have estimated unit vectors  $\hat{\mathbf{w}}_1, \dots, \hat{\mathbf{w}}_r$  and  $\hat{\mathbf{z}}_1, \dots, \hat{\mathbf{z}}_r$ . Then for given coefficients  $\hat{t}_1, \dots, \hat{t}_r$ , we define the estimator

$$\hat{\mathbf{A}} = \sum_{k=1}^r \hat{t}_k \hat{\mathbf{w}}_k \hat{\mathbf{z}}_k^T \quad (67)$$

We wish to find the values of  $\hat{t}_1, \dots, \hat{t}_r$  that minimize  $\|\mathbf{A} - \hat{\mathbf{A}}\|^2$ , and also to estimate  $\|\mathbf{A} - \hat{\mathbf{A}}\|^2$ . Let  $\mathbf{t} = (t_1, \dots, t_r)^T$  and  $\hat{\mathbf{t}} = (\hat{t}_1, \dots, \hat{t}_r)^T$ , and use “ $\odot$ ” to denote the Hadamard product between matrices. Then:

$$\begin{aligned} \|\mathbf{A} - \hat{\mathbf{A}}\|_F^2 &= \|\mathbf{W} \text{diag}(\mathbf{t}) \mathbf{Z}^T - \hat{\mathbf{W}} \text{diag}(\hat{\mathbf{t}}) \hat{\mathbf{Z}}^T\|_F^2 \\ &= \|\mathbf{W} \text{diag}(\mathbf{t}) \mathbf{Z}^T\|_F^2 + \|\hat{\mathbf{W}} \text{diag}(\hat{\mathbf{t}}) \hat{\mathbf{Z}}^T\|_F^2 - 2\langle \mathbf{W} \text{diag}(\mathbf{t}) \mathbf{Z}^T, \hat{\mathbf{W}} \text{diag}(\hat{\mathbf{t}}) \hat{\mathbf{Z}}^T \rangle_F \\ &= \mathbf{t}^T [(\mathbf{W}^T \mathbf{W}) \odot (\mathbf{Z}^T \mathbf{Z})] \mathbf{t} + \hat{\mathbf{t}}^T [(\hat{\mathbf{W}}^T \hat{\mathbf{W}}) \odot (\hat{\mathbf{Z}}^T \hat{\mathbf{Z}})] \hat{\mathbf{t}} - 2\hat{\mathbf{t}}^T [(\hat{\mathbf{W}}^T \mathbf{W}) \odot (\hat{\mathbf{Z}}^T \mathbf{Z})] \mathbf{t} \\ &= \mathbf{t}^T \mathbf{E} \mathbf{t} + \hat{\mathbf{t}}^T \mathbf{D} \hat{\mathbf{t}} - 2\hat{\mathbf{t}}^T \mathbf{C} \mathbf{t}, \end{aligned} \quad (68)$$

where  $\mathbf{E} = (\mathbf{W}^T \mathbf{W}) \odot (\mathbf{Z}^T \mathbf{Z})$ ,  $\mathbf{D} = (\hat{\mathbf{W}}^T \hat{\mathbf{W}}) \odot (\hat{\mathbf{Z}}^T \hat{\mathbf{Z}})$ , and  $\mathbf{C} = (\hat{\mathbf{W}}^T \mathbf{W}) \odot (\hat{\mathbf{Z}}^T \mathbf{Z})$ .

Written in this way, we see that the objective depends only on the inner products between the vectors  $\mathbf{w}_1, \dots, \mathbf{w}_r, \hat{\mathbf{w}}_1, \dots, \hat{\mathbf{w}}_r$ , and between the vectors  $\mathbf{z}_1, \dots, \mathbf{z}_r, \hat{\mathbf{z}}_1, \dots, \hat{\mathbf{z}}_r$ . Furthermore, we can reformulate the problem as another least-squares problem, with coefficients depending only on these inner products. Explicitly, if we write the Cholesky decomposition [20] of the positive definite matrix  $\mathbf{D}$  as

$$\mathbf{D} = \mathbf{M}^T \mathbf{M} \quad (69)$$

then it is easily checked that:

$$\|\mathbf{A} - \hat{\mathbf{A}}\|_F^2 = \|\mathbf{M} \hat{\mathbf{t}} - \mathbf{M}^{-T} \mathbf{C} \mathbf{t}\|_F^2 - \mathbf{t}^T [\mathbf{C}^T \mathbf{D}^{-1} \mathbf{C} - \mathbf{E}] \mathbf{t}. \quad (70)$$

This can be minimized by solving the least-squares problem

$$\hat{\mathbf{t}} = \underset{\hat{\mathbf{t}}'}{\text{argmin}} \|\mathbf{M} \hat{\mathbf{t}}' - \mathbf{M}^{-T} \mathbf{C} \mathbf{t}\|_F^2. \quad (71)$$

The error  $\|\mathbf{A} - \hat{\mathbf{A}}\|_F^2$  can then be evaluated by substituting  $\hat{\mathbf{t}}$  into (70).

## 4 Optimal spectral denoising with weighted loss

We use the theory developed in Section 3 to derive the optimal spectral denoising for weighted loss functions. In Section 4.1 we will perform the derivation for weighted Frobenius loss. In Section 4.2, we will show that under the weighted orthogonality condition on the signal singular vectors, there is a closed formula solution for the optimizing values. In Section 4.3, we will derive optimal spectral estimators for a more general family of weighted loss functions.

### 4.1 Weighted Frobenius loss

In this section, we derive the optimal singular value shrinker for weighted Frobenius loss. We restate the basic problem. We observe a  $p$ -by- $n$  matrix  $\mathbf{Y} = \mathbf{X} + \mathbf{G}$ , where  $\mathbf{X} = \sum_{k=1}^r t_k \mathbf{u}_k \mathbf{v}_k^T$ , and  $\mathbf{G}$  has iid entries

$G_{ij} \sim N(0, 1/n)$ . The top  $r$  singular vectors of  $\mathbf{Y}$  are denoted by  $\hat{\mathbf{u}}_1, \dots, \hat{\mathbf{u}}_r$  and  $\hat{\mathbf{v}}_1, \dots, \hat{\mathbf{v}}_r$ , and the singular values by  $\lambda_1, \dots, \lambda_r$ . Our goal is to find coefficients  $\hat{t}_1, \dots, \hat{t}_r$  so that the estimated matrix

$$\hat{\mathbf{X}} = \sum_{k=1}^r \hat{t}_k \hat{\mathbf{u}}_k \hat{\mathbf{v}}_k^T \quad (72)$$

minimizes the asymptotic weighted mean squared error, defined by

$$\text{AMSE}_\omega = \lim_{n \rightarrow \infty} \|\Omega(\hat{\mathbf{X}} - \mathbf{X})\Pi\|_F^2, \quad (73)$$

where  $p = p_n$  grows with  $n$ , and  $p/n \rightarrow \gamma$ , a finite constant.

We first make the simple observation that the weighted loss  $\|\Omega(\hat{\mathbf{X}} - \mathbf{X})\Pi\|_F^2$  between  $\hat{\mathbf{X}}$  and  $\mathbf{X}$  can be rewritten as the unweighted loss between  $\Omega\hat{\mathbf{X}}\Pi$  and  $\Omega\mathbf{X}\Pi$ . We can rewrite these matrices as follows:

$$\Omega\hat{\mathbf{X}}\Pi = \sum_{k=1}^r \hat{t}_k \Omega \hat{\mathbf{u}}_k (\Pi \hat{\mathbf{v}}_k)^T = \sum_{k=1}^r \hat{t}_k \|\Omega \hat{\mathbf{u}}_k\| \|\Pi \hat{\mathbf{v}}_k\| \hat{\mathbf{u}}_k^\omega (\hat{\mathbf{v}}_k^\omega)^T = \sum_{k=1}^r \hat{t}_k^\omega \hat{\mathbf{u}}_k^\omega (\hat{\mathbf{v}}_k^\omega)^T, \quad (74)$$

and

$$\Omega\mathbf{X}\Pi = \sum_{k=1}^r t_k \Omega \mathbf{u}_k (\Pi \mathbf{v}_k)^T = \sum_{k=1}^r t_k \sqrt{\alpha_k \beta_k} \mathbf{u}_k^\omega (\mathbf{v}_k^\omega)^T = \sum_{k=1}^r t_k^\omega \mathbf{u}_k^\omega (\mathbf{v}_k^\omega)^T, \quad (75)$$

where  $\hat{t}_k^\omega = \hat{t}_k \|\Omega \hat{\mathbf{u}}_k\| \|\Pi \hat{\mathbf{v}}_k\|$  and  $t_k^\omega = t_k \sqrt{\alpha_k \beta_k}$ .

Section 3.3 now tells us how to choose  $\hat{t}_k^\omega$  optimally, to minimize the Frobenius norm distance between  $\Omega\hat{\mathbf{X}}\Pi$  and  $\Omega\mathbf{X}\Pi$ . Specifically, defining  $c_{jk}^\omega, \tilde{c}_{jk}^\omega, d_{jk}, \tilde{d}_{jk}, e_{jk}$ , and  $\tilde{e}_{jk}$  as in formulas (43)–(45), we define the matrices

$$\mathbf{C} = \begin{pmatrix} c_{11}^\omega \tilde{c}_{11}^\omega & c_{12}^\omega \tilde{c}_{12}^\omega & \cdots & c_{1r}^\omega \tilde{c}_{1r}^\omega \\ c_{21}^\omega \tilde{c}_{21}^\omega & c_{22}^\omega \tilde{c}_{22}^\omega & \cdots & c_{2r}^\omega \tilde{c}_{2r}^\omega \\ \vdots & \vdots & \ddots & \vdots \\ c_{r1}^\omega \tilde{c}_{r1}^\omega & c_{r2}^\omega \tilde{c}_{r2}^\omega & \cdots & c_{rr}^\omega \tilde{c}_{rr}^\omega \end{pmatrix}, \quad (76)$$

$$\mathbf{D} = \begin{pmatrix} d_{11} \tilde{d}_{11} & d_{12} \tilde{d}_{12} & \cdots & d_{1r} \tilde{d}_{1r} \\ d_{21} \tilde{d}_{21} & d_{22} \tilde{d}_{22} & \cdots & d_{2r} \tilde{d}_{2r} \\ \vdots & \vdots & \ddots & \vdots \\ d_{r1} \tilde{d}_{r1} & d_{r2} \tilde{d}_{r2} & \cdots & d_{rr} \tilde{d}_{rr} \end{pmatrix}, \quad (77)$$

and

$$\mathbf{E} = \begin{pmatrix} e_{11} \tilde{e}_{11} & e_{12} \tilde{e}_{12} & \cdots & e_{1r} \tilde{e}_{1r} \\ e_{21} \tilde{e}_{21} & e_{22} \tilde{e}_{22} & \cdots & e_{2r} \tilde{e}_{2r} \\ \vdots & \vdots & \ddots & \vdots \\ e_{r1} \tilde{e}_{r1} & e_{r2} \tilde{e}_{r2} & \cdots & e_{rr} \tilde{e}_{rr} \end{pmatrix}. \quad (78)$$

Factoring  $\mathbf{D} = \mathbf{M}^T \mathbf{M}$ , the optimal vector  $\hat{\mathbf{t}}^\omega = (\hat{t}_1^\omega, \dots, \hat{t}_r^\omega)^T$  is the solution to the least squares problem

$$\hat{\mathbf{t}}^\omega = \underset{\mathbf{t}}{\text{argmin}} \|\mathbf{M}\mathbf{t} - \mathbf{M}^{-T} \mathbf{C} \mathbf{t}^\omega\|_F^2, \quad (79)$$

where  $\mathbf{t}^\omega = (t_1^\omega, \dots, t_r^\omega)^T$ . The optimal singular values  $\hat{t}_k$  are then defined by

$$\hat{t}_k = \frac{\hat{t}_k^\omega}{\|\Omega \hat{\mathbf{u}}_k\| \|\Pi \hat{\mathbf{v}}_k\|}, \quad 1 \leq k \leq r. \quad (80)$$

Furthermore, we can estimate the AMSE as

$$\text{AMSE}_\omega = \|\mathbf{M}\hat{\mathbf{t}}^\omega - \mathbf{M}^{-T} \mathbf{C} \mathbf{t}^\omega\|_F^2 - (\mathbf{t}^\omega)^T [\mathbf{C}^T \mathbf{D}^{-1} \mathbf{C} - \mathbf{E}] \mathbf{t}^\omega. \quad (81)$$

In order to solve the optimization problem (79) and evaluate the AMSE (81), we must estimate the parameters  $\alpha_k, \beta_k, c_{jk}^\omega, \tilde{c}_{jk}^\omega, d_{jk}, \tilde{d}_{jk}, e_{jk}$  and  $\tilde{e}_{jk}$ . We show how to do this in Section 4.1.1.

#### 4.1.1 Estimating $\alpha_k, \beta_k, c_{jk}^\omega, \tilde{c}_{jk}^\omega, d_{jk}, \tilde{d}_{jk}, e_{jk}$ and $\tilde{e}_{jk}$

First, from Proposition 3.1, we can estimate  $t_k$ ,  $c_k$  and  $\tilde{c}_k$ , so long as  $t_k > \gamma^{1/4}$ , i.e. if  $\lambda_k > 1 + \sqrt{\gamma}$ . Specifically,

$$t_k = \sqrt{\frac{\lambda_k^2 - 1 - \gamma + \sqrt{(\lambda_k^2 - 1 - \gamma)^2 - 4\gamma}}{2}}, \quad (82)$$

$$c_k = \sqrt{\frac{1 - \gamma/t_k^4}{1 + \gamma/t_k^2}}, \quad (83)$$

and

$$\tilde{c}_k = \sqrt{\frac{1 - \gamma/t_k^4}{1 + 1/t_k^2}}. \quad (84)$$

Next, we estimate  $\alpha_k$  and  $\beta_k$  using Proposition 3.2:

$$\alpha_k = \frac{\|\Omega \hat{\mathbf{u}}_k\|^2 - s_k^2 \mu}{c_k^2}, \quad (85)$$

and

$$\beta_k = \frac{\|\Pi \hat{\mathbf{v}}_k\|^2 - \tilde{s}_k^2 \nu}{\tilde{c}_k^2}. \quad (86)$$

The values  $d_{jk}$  and  $\tilde{d}_{jk}$  can be estimated directly, as they are inner products of empirical singular vectors. From Proposition 3.4, we can solve for  $e_{jk}$  and  $\tilde{e}_{jk}$ , so long as  $t_j$  and  $t_k$  both exceed  $\gamma^{1/4}$  (i.e.  $\lambda_j$  and  $\lambda_k$  both exceed  $1 + \sqrt{\gamma}$ ):

$$e_{jk} = d_{jk} \sqrt{\frac{c_j^2 \alpha_j + s_j^2 \mu}{c_j^2 \alpha_j} \cdot \frac{c_k^2 \alpha_k + s_k^2 \mu}{c_k^2 \alpha_k}}, \quad (87)$$

and

$$\tilde{e}_{jk} = \tilde{d}_{jk} \sqrt{\frac{\tilde{c}_j^2 \beta_j + \tilde{s}_j^2 \nu}{\tilde{c}_j^2 \beta_j} \cdot \frac{\tilde{c}_k^2 \beta_k + \tilde{s}_k^2 \nu}{\tilde{c}_k^2 \beta_k}}. \quad (88)$$

We can then use Proposition 3.3 to directly estimate  $c_{jk}^\omega$  and  $\tilde{c}_{jk}^\omega$ :

$$c_{jk}^\omega = e_{jk} \sqrt{\frac{c_j^2 \alpha_j}{c_j^2 \alpha_j + s_j^2 \mu}}, \quad (89)$$

and

$$\tilde{c}_{jk}^\omega = \tilde{e}_{jk} \sqrt{\frac{\tilde{c}_j^2 \beta_j}{\tilde{c}_j^2 \beta_j + \tilde{s}_j^2 \nu}}. \quad (90)$$

## 4.2 Separable denoisers under weighted orthogonality

The method we described in Section 4.1 makes no assumption on the singular vectors  $\mathbf{u}_k$  and  $\mathbf{v}_k$ . We find the entire vector  $\hat{\mathbf{t}}$  of  $\hat{t}_k$ 's as the solution of a least-squares problem. To obtain insight into the solution, however, it is convenient to have an analytic expression for the optimal  $\hat{t}_k$ .

In this section, we will impose the additional assumption that either  $\mathbf{u}_1, \dots, \mathbf{u}_r$  are asymptotically orthogonal with respect to  $\Omega^2$ , or that  $\mathbf{v}_1, \dots, \mathbf{v}_r$  are asymptotically orthogonal with respect to  $\Pi^2$ . Note that this is automatically satisfied if either  $\Omega = \mathbf{I}_p$  or  $\Pi = \mathbf{I}_n$ , that is, if the weights are only one-sided. It is also satisfied in the model where  $\mathbf{X}$  has iid columns, since then the  $\mathbf{v}_k$  are random vectors.

Under weighted orthogonality,  $e_{jk}\tilde{e}_{jk} = 0$  whenever  $j \neq k$ , and so  $d_{jk}\tilde{d}_{jk} = c_{jk}^\omega \tilde{c}_{jk}^\omega = 0$  when  $j \neq k$  as well. Consequently, the least squares problem (79) is a diagonal linear system, allowing us to solve for each  $\hat{t}_k^\omega$  independently. The solution is:

$$\hat{t}_k^\omega = t_k^\omega c_k^\omega \tilde{c}_k^\omega. \quad (91)$$

Consequently, the optimal  $\hat{t}_k$  is given by:

$$\begin{aligned} \hat{t}_k &= \frac{\hat{t}_k^\omega}{\|\Omega \hat{\mathbf{u}}_k\| \|\Pi \hat{\mathbf{v}}_k\|} \\ &= \frac{t_k^\omega c_k^\omega \tilde{c}_k^\omega}{\sqrt{(c_k^2 \alpha_k + s_k^2 \mu)(\tilde{c}_k^2 \beta_k + \tilde{s}_k^2 \nu)}} \\ &= t_k \sqrt{\alpha_k \beta_k} \sqrt{\frac{c_k^2 \alpha_k}{c_k^2 \alpha_k + s_k^2 \mu}} \sqrt{\frac{\tilde{c}_k^2 \beta_k}{\tilde{c}_k^2 \beta_k + \tilde{s}_k^2 \nu}} \frac{1}{\sqrt{(c_k^2 \alpha_k + s_k^2 \mu)(\tilde{c}_k^2 \beta_k + \tilde{s}_k^2 \nu)}} \\ &= t_k c_k \tilde{c}_k \cdot \frac{\alpha_k}{c_k^2 \alpha_k + s_k^2 \mu} \cdot \frac{\beta_k}{\tilde{c}_k^2 \beta_k + \tilde{s}_k^2 \nu}. \end{aligned} \quad (92)$$

The first term  $t_k c_k \tilde{c}_k$  is the optimal value with unweighted loss (as derived in [50, 19]). Using a weighted loss function necessitates multiplying this by the correction factor

$$\eta_k \equiv \frac{\alpha_k}{c_k^2 \alpha_k + s_k^2 \mu} \cdot \frac{\beta_k}{\tilde{c}_k^2 \beta_k + \tilde{s}_k^2 \nu}. \quad (93)$$

**Remark 2.** We observe that if both  $\mathbf{u}_k$  and  $\mathbf{v}_k$  are generic with respect to, respectively,  $\Omega^2$  and  $\Pi^2$  (in the sense defined in Section 1.4), then  $\alpha_k = \mu$  and  $\beta_k = \nu$ , and consequently  $\eta_k = 1$ . The optimal singular value  $\hat{t}_k$ , therefore, is equal to the optimal singular value for unweighted Frobenius loss. The optimal singular values depend not only on the choice of weights, but on the interaction between the weights and the singular vectors of  $\mathbf{X}$ .

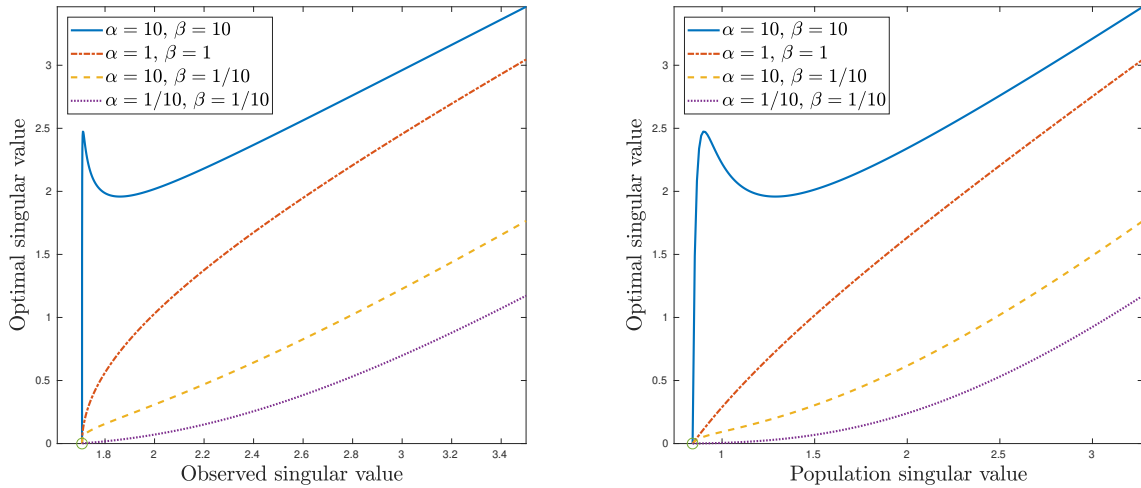


Figure 1: Optimal singular values  $\hat{t}$  plotted as functions of the observed singular values  $\lambda$  (left) and population singular values (right), for varying values of  $\alpha$  and  $\beta$  and  $\mu = \nu = 1$ .

#### 4.2.1 Magnitude of $\hat{t}$

When singular value denoising is used with unweighted loss functions, the optimal singular values are reduced in size from the observed singular values, in order to remove the effects of noise. Analyzing formula (92), we can see that for weighted loss functions, this need not be the case; if the loss function places weight on signal components that happen to be very strong, then the optimal singular values may be larger than the observed singular values. However, this can only occur when weights are placed on both the rows and coordinates – when only one dimension is weighted, the optimal singular values are, in fact, less than the observed values.

Suppose a coordinate has signal strength  $t = t_k$  (we drop the subscript as we are only considering one component). We may assume without loss of generality (and by rescaling  $\alpha$  and  $\beta$ ) that  $\mu = \nu = 1$ . Consequently, the optimal singular value is equal to:

$$\hat{t} = tc\tilde{c} \cdot \frac{\alpha}{c^2\alpha + s^2} \cdot \frac{\beta}{\tilde{c}^2\beta + \tilde{s}^2}. \quad (94)$$

By taking  $\alpha$  and  $\beta$  are sufficiently large, this value can be made arbitrarily close to

$$\frac{t}{c\tilde{c}} = \frac{t\sqrt{(1 + \gamma/t^2)(1 + 1/t^2)}}{1 - \gamma/t^4} = \frac{\lambda}{1 - \gamma/t^4} > \lambda. \quad (95)$$

That is, the optimal singular value  $\hat{t}$  will be greater than the observed singular value  $\lambda$  in this parameter regime.

On the other hand, if  $\beta \leq 1 = \nu$ , we have:

$$\frac{\hat{t}}{\lambda} = \frac{1}{\lambda} tc\tilde{c} \cdot \frac{\alpha}{c^2\alpha + s^2} \cdot \frac{\beta}{\tilde{c}^2\beta + \tilde{s}^2} \leq \frac{1}{\lambda} t \frac{\tilde{c}}{c} = \frac{t}{\sqrt{(t^2 + 1)(t^2 + \gamma)}} t \sqrt{\frac{t^2 + \gamma}{t^2 + 1}} = \frac{t^2}{t^2 + 1} \leq 1, \quad (96)$$

which shows that  $\hat{t} \leq \lambda$  always. A nearly identical proof works if  $\alpha \leq \mu$ .

We have shown:

**Proposition 4.1.** *If either  $\alpha_k \leq \mu$  or  $\beta_k \leq \nu$ , then  $\hat{t}_k \leq \lambda_k$ ; that is, the optimal singular value for weighted loss does not exceed the observed singular value. Conversely, for any fixed value of  $t_k$ , there are sufficiently large values of  $\alpha_k$  and  $\beta_k$  for which  $\hat{t}_k > \lambda_k$ .*

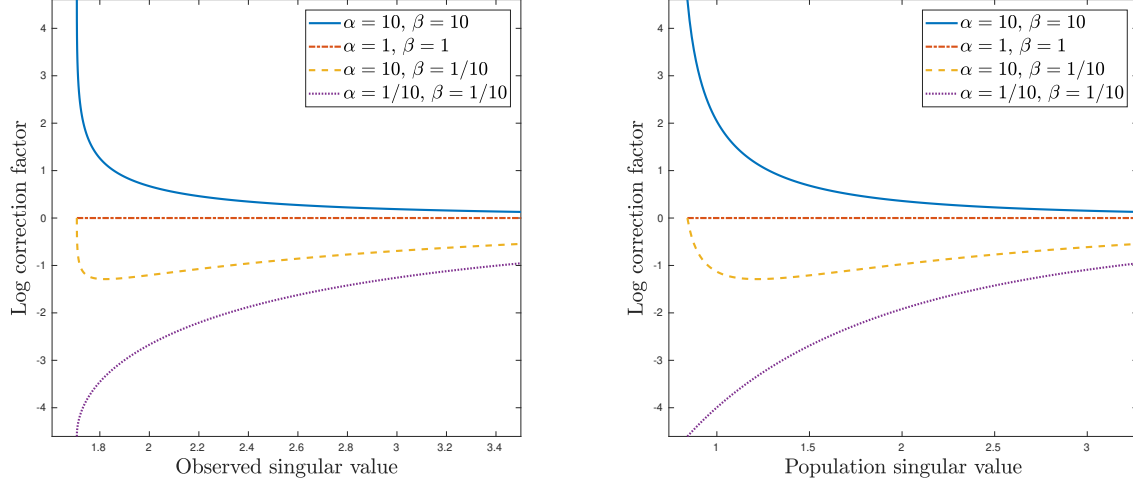


Figure 2: Log of the correction factor  $\eta$  plotted as functions of the observed singular values  $\lambda$  (left) and population singular values (right), for varying values of  $\alpha$  and  $\beta$  and  $\mu = \nu = 1$ .

#### 4.2.2 The correction factor $\eta$ and non-monotonicity of $\hat{t}$

Next, we examine some properties of the correction factor  $\eta = \eta_k$  defined in (93). Without loss of generality, we may assume  $\mu = \nu = 1$ . We have:

$$\frac{d}{dt} \frac{\alpha}{c^2\alpha + s^2} = \frac{\alpha(1-\alpha)}{[1+c^2(\alpha-1)]^2} \frac{dc^2}{dt}, \quad (97)$$

and

$$\frac{d}{dt} \frac{\beta}{\tilde{c}^2\beta + \tilde{s}^2} = \frac{\beta(1-\beta)}{[1+\tilde{c}^2(\beta-1)]^2} \frac{d\tilde{c}^2}{dt}. \quad (98)$$

Since  $c$  and  $\tilde{c}$  are both increasing functions of  $t$ , we see that so long as  $\alpha \leq \mu$  and  $\beta \leq \nu$ , the correction factor  $\eta = \eta(t)$  will be a monotonically increasing function of  $t$ , and so too will  $\hat{t}$ . However, if one or both of  $\alpha$  and/or  $\beta$  exceeds  $\mu$  or  $\nu$ , respectively, then the behavior of  $\eta$ , and consequently of  $\hat{t}$ , is not as simple. In particular, when  $\alpha$  and  $\beta$  are sufficiently large,  $\hat{t}$  need not increase monotonically with  $t$ .

To illustrate the behavior of  $\hat{t}$ , in Figure 1 we plot  $\hat{t}$ , both as a function of the observed singular value  $\lambda$  and the population singular value  $t$ , for various values of  $\alpha$  and  $\beta$  (and  $\mu = \nu = 1$ ). The non-monotonicity is apparent when  $\alpha = \beta = 10$ . In Figure 2, we plot the logarithm of the correction factors. We see that when  $\alpha = \beta = 10$ , the correction factor is a decreasing function of  $\lambda$  (equivalently, of  $t$ ), which explains the non-monotonicity of  $\hat{t}$ . Furthermore, the behavior when  $\alpha = 10$  and  $\beta = 1$  is non-monotonic; the function decreases, and then increases.

### 4.3 Other weighted loss functions

The paper [19] considers a wide range of orthogonally-invariant, block-decomposable loss functions, such as the Schatten  $p$ -norms (which include the nuclear norm and operator norm as a special case). We can extend our method to handle weighted versions of these loss functions, namely

$$\mathcal{L}_\omega(\hat{\mathbf{X}}, \mathbf{X}) = \mathcal{L}(\Omega\hat{\mathbf{X}}\Pi, \Omega\mathbf{X}\Pi), \quad (99)$$

where  $\mathcal{L}$  is orthogonally-invariant and block-decomposable. We require the weighted orthogonality condition, namely that both the singular vectors  $\mathbf{u}_1, \dots, \mathbf{u}_r$  are asymptotically orthogonal with respect to  $\Omega^2$ , and  $\mathbf{v}_1, \dots, \mathbf{v}_r$  are asymptotically orthogonal with respect to  $\Pi^2$ . Equivalently,  $e_{jk} = \tilde{e}_{jk} = 0$  whenever  $j \neq k$ ; it follows that  $\mathbf{u}_1^\omega, \dots, \mathbf{u}_r^\omega$  are also pairwise orthogonal, as are  $\hat{\mathbf{v}}_1^\omega, \dots, \hat{\mathbf{v}}_r^\omega$ .

Under weighted orthogonality, the same analysis carried out in [19] goes through verbatim to the two weighted matrices  $\Omega\hat{\mathbf{X}}\Pi$  and  $\Omega\mathbf{X}\Pi$ . Specifically, there are coordinate systems of the row and column spaces in which  $\Omega\hat{\mathbf{X}}\Pi$  and  $\Omega\mathbf{X}\Pi$  consist of  $r$  2-by-2 blocks. More precisely, there are orthogonal matrices  $\mathbf{A}$  and  $\mathbf{B}$  such that  $\mathbf{A}(\Omega\hat{\mathbf{X}}\Pi)\mathbf{B}^T = \bigoplus_{k=1}^r \hat{t}_k^\omega \mathbf{C}_k$  and  $\mathbf{A}(\Omega\mathbf{X}\Pi)\mathbf{B}^T = \bigoplus_{k=1}^r \mathbf{D}_k$ , where

$$\mathbf{C}_k = \begin{pmatrix} c_k^\omega \tilde{c}_k^\omega & c_k^\omega \tilde{s}_k^\omega \\ \tilde{c}_k^\omega s_k^\omega & s_k^\omega \tilde{s}_k^\omega \end{pmatrix}, \quad (100)$$

and

$$\mathbf{D}_k = t_k^\omega \begin{pmatrix} 1 & 0 \\ 0 & 0 \end{pmatrix}. \quad (101)$$

For each  $1 \leq k \leq r$ , the optimal  $\hat{t}_k^\omega$  is then a solution to the optimization problem:

$$\hat{t}_k^\omega = \operatorname{argmin}_t \mathcal{L}(t\mathbf{C}_k, \mathbf{D}_k). \quad (102)$$

For nuclear norm and operator norm loss, there is a closed form solution; for other loss functions, the solution may be obtained by a straightforward numerical optimization. We refer the reader to [19] for details. Having found the optimal  $\hat{t}_k^\omega$ , we then define  $\hat{t}_k = \hat{t}_k^\omega / (\|\Omega\hat{\mathbf{u}}_k\| \|\Pi\hat{\mathbf{v}}_k\|)$ .

## 5 Localized matrix denoising for unweighted loss

In Section 4, we derived optimal spectral estimators for estimating  $\mathbf{X}$  with respect to a specified weighted loss function. In this section, we revisit ordinary, unweighted Frobenius loss. Because the noise matrix  $\mathbf{G}$  is isotropic and unweighted Frobenius loss is orthogonally-invariant, singular value shrinkage is known to be the optimal method in this setting, both in the minimax sense and when averaging over a uniform prior on the  $\mathbf{u}_k$  and  $\mathbf{v}_k$  [17, 50]. In this section, we will show that there are other procedures that outperform singular value shrinkage.

The central idea is that by combining different choices of weight matrices that tile all of  $\mathbb{R}^{p \times n}$ , we may denoise different regions of  $\mathbf{X}$  optimally, and achieve a smaller overall error. In Section 5.1 we derive this new method, which we call *localized matrix denoising*. We will prove that it is never worse than global singular value shrinkage. In Section 5.2, we will show that if the singular vectors of  $\mathbf{X}$  are heterogeneous with respect to the projection matrices used to define the local denoiser, the local denoising is strictly better than global shrinkage.

If  $\mathbf{X}$  contains submatrices that vary in signal strength, a natural question is whether we should combine the submatrices into one matrix at all – perhaps we would do better by applying shrinkage to a given submatrix individually. We address this in Section 5.3. Specifically, we show that so long as any one submatrix is not too dominant, we achieve more accurate estimation of its singular vectors by merging it with the other submatrices and projecting, rather than computing its singular vectors alone.

### 5.1 Description of localized denoising

We now introduce localized denoising. We take any two expansions of the identity matrices  $\mathbf{I}_p$  and  $\mathbf{I}_n$  into sums of pairwise orthogonal projection matrices  $\Omega_i$  and  $\Pi_j$ :

$$\mathbf{I}_p = \sum_{i=1}^I \Omega_i \quad (103)$$

and

$$\mathbf{I}_n = \sum_{j=1}^J \Pi_j. \quad (104)$$

We let  $\widehat{\mathbf{X}}_{(i,j)}^{\text{loc}}$  denote the optimally denoised matrix with respect to the weight matrices  $\Omega_i$  and  $\Pi_j$ . We then define the locally-denoised matrix:

$$\widehat{\mathbf{X}}^{\text{loc}} = \sum_{i=1}^I \sum_{j=1}^J \Omega_i \widehat{\mathbf{X}}_{(i,j)}^{\text{loc}} \Pi_j. \quad (105)$$

We will denote by  $\widehat{\mathbf{X}}^{\text{shr}} = \sum_{k=1}^r t_k c_k \tilde{c}_k \hat{\mathbf{u}}_k \hat{\mathbf{v}}_k^T$  the matrix that is optimally shrunk with respect to ordinary Frobenius loss. We then have the following result:

**Proposition 5.1.** *For any choice of pairwise orthogonal projections  $\Omega_i$  and  $\Pi_j$  satisfying (103) and (104), the AMSE of  $\widehat{\mathbf{X}}^{\text{loc}}$  does not exceed the AMSE of  $\widehat{\mathbf{X}}^{\text{shr}}$ . That is,*

$$\|\widehat{\mathbf{X}}^{\text{loc}} - \mathbf{X}\|_F^2 \leq \|\widehat{\mathbf{X}}^{\text{shr}} - \mathbf{X}\|_F^2, \quad (106)$$

where the inequality holds almost surely as  $p, n \rightarrow \infty$ .

*Proof.* We denote by  $\hat{t}_1^{\text{shr}}, \dots, \hat{t}_r^{\text{shr}}$  the singular values of  $\widehat{\mathbf{X}}^{\text{shr}}$ . We then have:

$$\widehat{\mathbf{X}}^{\text{shr}} = \sum_{i=1}^I \sum_{j=1}^J \sum_{k=1}^r \hat{t}_k^{\text{shr}} (\Omega_i \hat{\mathbf{u}}_k) (\Pi_j \hat{\mathbf{v}}_k)^T. \quad (107)$$

Writing  $\mathbf{X}_{(i,j)} = \Omega_i \mathbf{X} \Pi_j$ , we can decompose the loss between  $\widehat{\mathbf{X}}^{\text{shr}}$  and  $\mathbf{X}$  as follows:

$$\|\widehat{\mathbf{X}}^{\text{shr}} - \mathbf{X}\|_{\text{F}}^2 = \sum_{i=1}^I \sum_{j=1}^J \left\| \sum_{k=1}^r \widehat{t}_k^{\text{shr}} (\Omega_i \hat{\mathbf{u}}_k) (\Pi_j \hat{\mathbf{v}}_k)^T - \mathbf{X}_{(i,j)} \right\|_{\text{F}}^2. \quad (108)$$

On the other hand, we can write

$$\widehat{\mathbf{X}}^{\text{loc}} = \sum_{i=1}^I \sum_{j=1}^J \sum_{k=1}^r \widehat{t}_k^{(i,j)} (\Omega_i \hat{\mathbf{u}}_k) (\Pi_j \hat{\mathbf{v}}_k)^T, \quad (109)$$

where  $\hat{\mathbf{t}}^{(i,j)} = (\widehat{t}_1^{(i,j)}, \dots, \widehat{t}_r^{(i,j)})^T$  is defined by

$$\hat{\mathbf{t}}^{(i,j)} = \underset{(\hat{t}_1, \dots, \hat{t}_r)^T}{\text{argmin}} \left\| \Omega_i \left( \sum_{k=1}^r \hat{t}_k \hat{\mathbf{u}}_k \hat{\mathbf{v}}_k^T - \mathbf{X} \right) \Pi_j \right\|_{\text{F}}^2 = \underset{(\hat{t}_1, \dots, \hat{t}_r)^T}{\text{argmin}} \left\| \sum_{k=1}^r \hat{t}_k (\Omega_i \hat{\mathbf{u}}_k) (\Pi_j \hat{\mathbf{v}}_k)^T - \Omega_i \mathbf{X} \Pi_j \right\|_{\text{F}}^2. \quad (110)$$

Consequently, for all  $i$  and  $j$ :

$$\left\| \sum_{k=1}^r \widehat{t}_k^{(i,j)} (\Omega_i \hat{\mathbf{u}}_k) (\Pi_j \hat{\mathbf{v}}_k)^T - \mathbf{X}_{(i,j)} \right\|_{\text{F}}^2 \leq \left\| \sum_{k=1}^r \widehat{t}_k^{\text{shr}} (\Omega_i \hat{\mathbf{u}}_k) (\Pi_j \hat{\mathbf{v}}_k)^T - \mathbf{X}_{(i,j)} \right\|_{\text{F}}^2 \quad (111)$$

from which it follows that:

$$\begin{aligned} \|\widehat{\mathbf{X}}^{\text{loc}} - \mathbf{X}\|_{\text{F}}^2 &= \sum_{i=1}^I \sum_{j=1}^J \left\| \sum_{k=1}^r \widehat{t}_k^{(i,j)} (\Omega_i \hat{\mathbf{u}}_k) (\Pi_j \hat{\mathbf{v}}_k)^T - \mathbf{X}_{(i,j)} \right\|_{\text{F}}^2 \\ &\leq \sum_{i=1}^I \sum_{j=1}^J \left\| \sum_{k=1}^r \widehat{t}_k^{\text{shr}} (\Omega_i \hat{\mathbf{u}}_k) (\Pi_j \hat{\mathbf{v}}_k)^T - \mathbf{X}_{(i,j)} \right\|_{\text{F}}^2 = \|\widehat{\mathbf{X}}^{\text{shr}} - \mathbf{X}\|_{\text{F}}^2, \end{aligned} \quad (112)$$

which is the desired inequality.  $\square$

## 5.2 Localized denoising with heterogeneous signals

Proposition 5.1 tells us that localized denoising is never worse than global singular value shrinkage. In this section, we will show that if the signal matrix's singular vectors are heterogeneous with respect to the projections  $\Omega_i$  or  $\Pi_j$ , localized denoising is strictly better than global shrinkage. We will consider the case where we subdivide one dimension of the matrix, which without loss of generality we take to be the rows.

Let  $\mathbf{u}_k^{(i)} = \Omega_i \mathbf{u}_k / \|\Omega_i \mathbf{u}_k\|$ ,  $i = 1, \dots, I$  and  $k = 1, \dots, r$ . Because the column weights are uniform, we may use the separable shrinkage procedure described in Section 4.2. The optimal singular values  $\widehat{t}_k^{(i)}$  for denoising with the weight matrix  $\Omega_i$  are given by

$$\widehat{t}_k^{(i)} = t_k c_k \tilde{c}_k \cdot \frac{\alpha_k^{(i)}}{c_k^2 \alpha_k^{(i)} + s_k^2 \mu^{(i)}}, \quad (113)$$

where  $\alpha_k^{(i)} = \|\Omega_i \mathbf{u}_k\|^2$  and  $\mu^{(i)} = \text{tr}(\Omega_i^2)/p$ .

On the other hand, the singular values of  $\widehat{\mathbf{X}}$  are  $\widehat{t}_k^{\text{shr}} = t_k c_k \tilde{c}_k$ . From inequalities (111) and (112),  $\widehat{\mathbf{X}}^{\text{loc}}$  will have strictly smaller loss than  $\widehat{\mathbf{X}}^{\text{shr}}$  whenever  $\widehat{t}_k^{(i)} \neq \widehat{t}_k^{\text{shr}}$  for some  $i$  and some  $k$ . This can only fail when  $\alpha_k^{(i)} = \mu^{(i)}$  for all  $i$  and  $k$ ; that is, when each component  $\mathbf{u}_k$  is generic with respect to each projection  $\Omega_i$ .

We have shown the following result:

**Proposition 5.2.** *If any left singular vectors  $\mathbf{u}_k$  of  $\mathbf{X}$  is heterogeneous with respect to some projection  $\Omega_i$ , than the AMSE for local denoising with  $\Omega_1, \dots, \Omega_I$  will be strictly smaller than the AMSE for global shrinkage:*

$$\lim_{n \rightarrow \infty} \|\widehat{\mathbf{X}}^{\text{loc}} - \mathbf{X}\|_{\text{F}}^2 < \lim_{n \rightarrow \infty} \|\widehat{\mathbf{X}}^{\text{shr}} - \mathbf{X}\|_{\text{F}}^2, \quad (114)$$

where the limits hold almost surely as  $p, n \rightarrow \infty$  and  $p/n \rightarrow \gamma$ .

### 5.3 Matrix splitting versus localized denoising

In this section, we consider an alternative procedure to localized shrinkage for heterogeneous signals. Suppose  $\mathbf{I}_p = \sum_{i=1}^I \Omega_i$ , where the  $\Omega_i$  are pairwise orthogonal projection matrices. We consider the task of denoising one of the submatrices  $\mathbf{X}_0 = \mathbf{X}_{(i_0)} = \Omega_{i_0} \mathbf{X}$ . One method is to apply localized denoising to the entire observed matrix  $\mathbf{Y}$ , yielding the estimator  $\widehat{\mathbf{X}}^{\text{loc}} = \sum_{k=1}^r \hat{t}_k \hat{\mathbf{u}}_k \hat{\mathbf{v}}_k^T$ , and then restrict to the submatrix  $\widehat{\mathbf{X}}_0^{\text{loc}} = \Omega_{i_0} \widehat{\mathbf{X}}^{\text{loc}}$ . This is of the form:

$$\widehat{\mathbf{X}}_0^{\text{loc}} = \sum_{k=1}^r \hat{t}_k \Omega_{i_0} \hat{\mathbf{u}}_k \hat{\mathbf{v}}_k^T = \sum_{k=1}^r \hat{t}_k^\omega \hat{\mathbf{u}}_k^\omega \hat{\mathbf{v}}_k^T, \quad (115)$$

where  $\hat{\mathbf{u}}_k$  and  $\hat{\mathbf{v}}_k$  are the singular vectors of the whole data matrix  $\mathbf{Y}$ , and  $\hat{\mathbf{u}}_k^\omega = \Omega_{i_0} \hat{\mathbf{u}}_k / \|\Omega_{i_0} \hat{\mathbf{u}}_k\|$ . We will assume the weighted orthogonality condition on the  $\mathbf{u}_k$  with respect to  $\Omega_{i_0}$ , implying that the vectors  $\mathbf{u}_k^\omega = \Omega_{i_0} \mathbf{u}_k / \|\Omega_{i_0} \mathbf{u}_k\|$  are asymptotically pairwise orthogonal, and so are the  $\hat{\mathbf{u}}_k^\omega$ . Consequently, (115) is an SVD of  $\widehat{\mathbf{X}}_0^{\text{loc}}$ .

Alternatively, we might choose to ignore the other regions of the observed matrix  $\mathbf{Y}_{(i)}$ ,  $i \neq i_0$ , and perform singular value shrinkage to the submatrix  $\mathbf{Y}_0 = \mathbf{Y}_{(i_0)} = \mathbf{X}_0 + \mathbf{G}_0$ ; in other words, we may *split*  $\mathbf{Y}_0$  from the full observed matrix  $\mathbf{Y}$ , and optimally shrink its singular values. Let us denote by  $\widehat{\mathbf{X}}_0^{\text{spl}}$  the resulting estimate of  $\mathbf{X}_0$ .

Which procedure performs better,  $\widehat{\mathbf{X}}_0^{\text{loc}}$  or  $\widehat{\mathbf{X}}_0^{\text{spl}}$ ? Let  $\alpha_k = \|\Omega_i \mathbf{u}_k\|^2$ , and  $\mathbf{u}_k^\omega = \Omega_i \mathbf{u}_k / \|\Omega_i \mathbf{u}_k\|$ . Then the submatrix  $\mathbf{X}_0$  can be written as

$$\mathbf{X}_0 = \Omega_{i_0} \sum_{k=1}^r t_k \mathbf{u}_k \mathbf{v}_k^T = \sum_{k=1}^r t_k^\omega \mathbf{u}_k^\omega \mathbf{v}_k^T, \quad (116)$$

where  $t_k^\omega = t_k \sqrt{\alpha_k}$ , and  $\mathbf{u}_k^\omega = \Omega_{i_0} \mathbf{u}_k / \|\Omega_{i_0} \mathbf{u}_k\|$ . Under the weighted orthogonality condition, (116) is the SVD of  $\mathbf{X}_0$ . If  $\mathbf{Y}_0 = \Omega_i \mathbf{Y} = \mathbf{X}_0 + \mathbf{G}_0$  is the observed submatrix of  $\mathbf{Y}$ , and  $\hat{\mathbf{u}}_1^0, \dots, \hat{\mathbf{u}}_r^0$  and  $\hat{\mathbf{v}}_1^0, \dots, \hat{\mathbf{v}}_r^0$  are its top  $r$  left and right singular vectors, respectively, then

$$\widehat{\mathbf{X}}_0^{\text{spl}} = \sum_{k=1}^r t_k^0 \hat{\mathbf{u}}_k^0 (\hat{\mathbf{v}}_k^0)^T, \quad (117)$$

where  $t_k^0 = t_k \sqrt{\alpha_k} c_k^0 \tilde{c}_k^0$ ,  $c_k^0 = |\langle \mathbf{u}_k^\omega, \hat{\mathbf{u}}_k^0 \rangle|$  and  $\tilde{c}_k^0 = |\langle \mathbf{v}_k, \hat{\mathbf{v}}_k^0 \rangle|$ .

The estimator  $\widehat{\mathbf{X}}_0^{\text{loc}}$  will perform better than  $\widehat{\mathbf{X}}_0^{\text{spl}}$  if its singular vectors  $\hat{\mathbf{u}}_k^\omega$  and  $\hat{\mathbf{v}}_k$  are closer to the singular vectors of  $\mathbf{X}_0$ ,  $\mathbf{u}_k^\omega$  and  $\mathbf{v}_k$ , than are the singular vectors  $\hat{\mathbf{u}}_k^0$  and  $\hat{\mathbf{v}}_k^0$  of  $\widehat{\mathbf{X}}_0^{\text{spl}}$ . We show that this occurs when the subvector  $\Omega_{i_0} \mathbf{u}_k$  does not contain too much of the energy of  $\mathbf{u}_k$ . More precisely, we have:

**Proposition 5.3.** *For  $1 \leq k \leq r$ , if  $\alpha_k \leq \sqrt{\mu}$  then*

$$|\langle \hat{\mathbf{u}}_k^0, \mathbf{u}_k^\omega \rangle| \leq |\langle \hat{\mathbf{u}}_k^\omega, \mathbf{u}_k^\omega \rangle|, \quad (118)$$

and

$$|\langle \hat{\mathbf{v}}_k^0, \mathbf{v}_k \rangle| \leq |\langle \hat{\mathbf{v}}_k, \mathbf{v}_k \rangle|, \quad (119)$$

where the inequalities hold almost surely in the limit  $p, n \rightarrow \infty$ . Consequently,

$$\|\widehat{\mathbf{X}}_0^{\text{loc}} - \mathbf{X}_0\|_F^2 \leq \|\widehat{\mathbf{X}}_0^{\text{spl}} - \mathbf{X}_0\|_F^2 \quad (120)$$

almost surely in the limit  $p, n \rightarrow \infty$ .

**Remark 3.** Informally, Proposition 5.3 tells us that as long as the signal is not too concentrated on  $\mathbf{X}_0$ , we will obtain a better estimate of the singular vectors of  $\mathbf{X}_0$  by computing the singular vectors of the full matrix  $\mathbf{Y}$  and projecting onto the coordinates of interest, instead of using the singular vectors of the submatrix  $\mathbf{Y}_0$  alone. Phrased differently, the other blocks of the matrix boost the signal in  $\mathbf{Y}_0$ .

**Remark 4.** If the signal vector  $\mathbf{u}_k$  is generic, then  $\alpha = \mu < 1$ ; so the bound of this proposition says that even a strongly heterogeneous block of the matrix benefits by including other regions of the matrix in the denoising procedure.

*Proof of Proposition 5.3.* We let  $q = \text{tr}(\Omega_i)$  be the dimension of the projected subspace. We will, by abuse of notation, say that matrices of the form  $\Omega_i \mathbf{A}$  have  $q$  rows, so that  $\mathbf{X}_0$ ,  $\mathbf{Y}_0$ ,  $\widehat{\mathbf{X}}_0^{\text{spl}}$  and  $\widehat{\mathbf{X}}_0^{\text{loc}}$  all lie in  $\mathbb{R}^{q \times n}$ . Setting  $\mu = \text{tr}(\Omega_i^2)/p$ , we have  $q = p\mu$ ; then the aspect ratio of  $\mathbf{X}_0$  is  $\gamma_0 = \mu\gamma$ , and  $\mathbf{X}_0$  has singular values  $t_k\sqrt{\alpha_k}$ . Since we only analyze one component at a time, we will drop the subscript  $k$ .

Let  $R = \gamma/t^4$ . Note that if  $R > 1$ , then  $t^4 < \gamma$ , and so if  $\alpha < \sqrt{\mu}$ , then  $t^4\alpha^2 < \mu\gamma$ , so the signal is not detectable from  $\mathbf{Y}_0$ ; that is,  $\langle \hat{\mathbf{u}}^0, \mathbf{u}^\omega \rangle \sim 0$  and  $\langle \hat{\mathbf{v}}^0, \mathbf{v} \rangle \sim 0$ . Consequently, we may assume  $0 < R \leq 1$ . We first show  $|\langle \hat{\mathbf{u}}^0, \mathbf{u}^\omega \rangle| \leq |\langle \hat{\mathbf{u}}^\omega, \mathbf{u}^\omega \rangle|$ . Observe that

$$\langle \hat{\mathbf{u}}^0, \mathbf{u}^\omega \rangle^2 \sim \frac{1 - (\mu\gamma)/(\alpha^2 t^4)}{1 + (\mu\gamma)/(\alpha t^2)} = \frac{\alpha^2 - \mu R}{\alpha^2 + \alpha t^2 \mu R}. \quad (121)$$

From Section 3.1, we know that

$$\langle \hat{\mathbf{u}}^\omega, \mathbf{u}^\omega \rangle^2 \sim \frac{c^2 \alpha}{c^2 \alpha + s^2 \mu} \quad (122)$$

where

$$c^2 = \frac{1 - \gamma/t^4}{1 + \gamma/t^2} = \frac{1 - R}{1 + t^2 R} \quad (123)$$

and

$$s^2 = 1 - c^2 = \frac{R + t^2 R}{1 + t^2 R}. \quad (124)$$

Multiplying numerator and denominator by  $\alpha(1 + t^2 R)$ , this expression can be rewritten:

$$\langle \hat{\mathbf{u}}^\omega, \mathbf{u}^\omega \rangle^2 \sim \frac{c^2 \alpha}{c^2 \alpha + s^2 \mu} = \frac{(1 - R)\alpha^2}{(1 - R)\alpha^2 + (R + t^2 R)\mu\alpha} = \frac{\alpha^2 - \mu R + R(\mu - \alpha^2)}{\alpha^2 + \alpha t^2 \mu R + R\alpha(\mu - \alpha)}. \quad (125)$$

From (121) and (125), the inequality

$$|\langle \hat{\mathbf{u}}^0, \mathbf{u}^\omega \rangle| \leq |\langle \hat{\mathbf{u}}^\omega, \mathbf{u}^\omega \rangle| \quad (126)$$

is equivalent to

$$R\alpha(\mu - \alpha)(\alpha^2 - \mu R) \leq R(\mu - \alpha^2)(\alpha^2 + \alpha t^2 \mu R) \quad (127)$$

which can be simplified to the inequality

$$R(\alpha - \mu + t^2(\alpha^2 - \mu)) - \alpha(1 - \alpha) \leq 0. \quad (128)$$

Since this expression is affine linear in  $R$ , and  $0 < R \leq 1$ , it is enough to check that the inequality holds when  $R = 0$  and  $R = 1$ . When  $R = 0$ , the left side is  $\alpha(\alpha - 1)$ , which is negative since  $\alpha < 1$ . When  $R = 1$ , the left side can be rewritten as

$$\alpha - \mu + t^2(\alpha^2 - \mu) - \alpha + \alpha^2 = (t^2 + 1)\alpha^2 - (t^2 + 1)\mu = (t^2 + 1)(\alpha^2 - \mu), \quad (129)$$

which is negative since  $\alpha < \sqrt{\mu}$ . This completes the proof that  $|\langle \hat{\mathbf{u}}^0, \mathbf{u}^\omega \rangle| \leq |\langle \hat{\mathbf{u}}^\omega, \mathbf{u}^\omega \rangle|$ .

Next we show that  $|\langle \hat{\mathbf{v}}^0, \mathbf{v} \rangle| \leq |\langle \hat{\mathbf{v}}, \mathbf{v} \rangle|$ . Since  $\mathbf{Y}_0$  has aspect ratio  $\mu\gamma$ , and  $\mathbf{X}_0$  has signal strength  $t\sqrt{\alpha}$ , we have

$$|\langle \hat{\mathbf{v}}^0, \mathbf{v} \rangle| \sim \frac{1 - (\mu\gamma)/(\alpha^2 t^4)}{1 + 1/(\alpha t^2)} = \frac{\alpha^2 t^4 - \mu\gamma}{\alpha^2 t^4 + \alpha t^2}, \quad (130)$$

and

$$|\langle \hat{\mathbf{v}}, \mathbf{v} \rangle| \sim \frac{1 - \gamma/t^4}{1 + 1/t^2} = \frac{t^4 - \gamma}{t^4 + t^2}. \quad (131)$$

The inequality  $|\langle \hat{\mathbf{v}}^0, \mathbf{v} \rangle| \leq |\langle \hat{\mathbf{v}}, \mathbf{v} \rangle|$  is therefore equivalent to showing that

$$\frac{\alpha^2 t^4 - \mu\gamma}{\alpha^2 t^2 + \alpha} \leq \frac{t^4 - \gamma}{t^2 + 1}, \quad (132)$$

or equivalently

$$h(\alpha) \equiv \alpha^2 \left( \frac{t^4 - \gamma}{t^2 + 1} t^2 - t^4 \right) + \alpha \frac{t^4 - \gamma}{t^2 + 1} + \mu\gamma \geq 0. \quad (133)$$

The quadratic polynomial  $h(\alpha)$  has negative leading term;  $h(0) = \mu\gamma > 0$ ; and

$$h(\sqrt{\mu}) \geq \mu \left( \frac{t^4 - \gamma}{t^2 + 1} t^2 - t^4 \right) + \mu \frac{t^4 - \gamma}{t^2 + 1} + \mu\gamma = \mu \left( \frac{t^4 - \gamma}{t^2 + 1} \right) (t^2 + 1) - \mu(t^4 - \gamma) = 0. \quad (134)$$

Consequently,  $h(\alpha) \geq 0$  for all  $0 \leq \alpha \leq \sqrt{\mu}$ , completing the proof.  $\square$

## 6 Numerical results

We report on numerical simulations that illustrate the theoretical results from the paper. In Section 6.1, we illustrate the weighted singular value denoising method on missing data, as described in Section 2.2. In Section 6.2, we illustrate weighted singular value denoising on doubly-heteroscedastic noise, as described in Section 2.1.

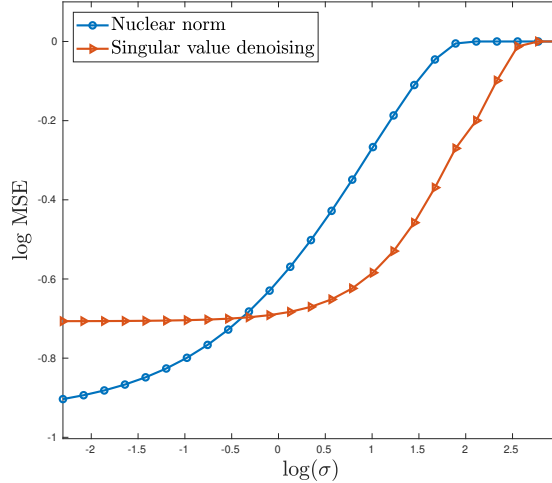


Figure 3: Optimal singular value denoising versus nuclear norm regularized least squares.

### 6.1 Missing data

In this experiment, we test the performance of singular value denoising on a missing data problem, following the procedure described in Section 2.2. We compare our method to nuclear-norm regularized least-squares [9], which estimates  $\mathbf{X}$  by:

$$\hat{\mathbf{X}}^{\text{nuc}} = \underset{\hat{\mathbf{X}} \in \mathbb{R}^{p \times n}}{\text{argmin}} \left\{ \frac{1}{2} \|\mathcal{F}(\hat{\mathbf{X}}) - \mathbf{y}\|^2 + \lambda \|\mathbf{P}^{1/2} \hat{\mathbf{X}} \mathbf{Q}^{1/2}\|_* \right\}. \quad (135)$$

Table 1: Cosines between empirical and population vectors — missing data

$m$	Bias inner	Bias outer	Error inner	Error outer
500	-9.64e-03	-9.82e-03	2.20e-02	2.15e-02
1000	-4.89e-03	-4.86e-03	1.43e-02	1.38e-02
2000	-2.35e-03	-2.35e-03	9.42e-03	9.13e-03
4000	-1.23e-03	-1.20e-03	6.47e-03	6.19e-03
8000	-6.18e-04	-6.16e-04	4.48e-03	4.33e-03

Here,  $\|\cdot\|_*$  denotes the nuclear norm,  $\mathcal{F} : \mathbb{R}^{p \times n} \rightarrow \mathbb{R}^M$  is the projection operator onto the  $M$  observed samples, and  $\mathbf{P}$  and  $\mathbf{Q}$  are the diagonal matrices of sampling probabilities for rows and columns, respectively. We weight the nuclear norm by the square root of the sampling probabilities, as is suggested in [11]. Following [9], we choose the parameter  $\lambda$  so that when  $\mathbf{y}$  is pure noise,  $\widehat{\mathbf{X}}^{\text{nuc}}$  is set to zero. It follows from the KKT conditions for the problem [8] that this is equivalent to:

$$\lambda = \|\mathbf{P}^{-1/2} \mathcal{F}^*(\mathbf{y}) \mathbf{Q}^{-1/2}\|_*. \quad (136)$$

Since the matrix  $\mathbf{P}^{-1/2} \mathcal{F}^*(\mathbf{y}) \mathbf{Q}^{-1/2}$  has independent entries with variance 1, we may set  $\lambda = 1 + \sqrt{\gamma}$ . We solve the minimization (135) using the algorithm in [29].

We generate a rank 5 signal matrix  $\mathbf{X}$  of size 200-by-400, and a Gaussian noise matrix  $\mathbf{G}$  of the same dimension, where each entry has variance  $\sigma^2$  for a specified value of  $\sigma$ . We subsample the matrix  $\mathbf{X} + \mathbf{G}$  using row sampling probabilities linearly spaced between .3 and .7, and linearly-spaced column sampling probabilities with the same range.

For different values of  $\sigma$ , we repeat the experiment 10000 times and average the errors. In Figure 3, we plot the logarithm of the error against  $\log(\sigma)$ . We observe that when  $\sigma$  is large, singular value denoising performs substantially better than nuclear-norm regularized least-squares. However, in the small  $\sigma$  regime, the reverse is true. This is consistent with the experimental results from [14].

**Remark 5.** We note that the error curve for the spectral denoiser in Figure 3 has a slight “dent” at large  $\sigma$ . This is due to the instability of rank estimation in low SNR. In our experiment, we keep the components whose singular values exceed the bulk edge  $1 + \sqrt{\gamma}$  plus a small correction factor  $\epsilon$ ; in future work a more principled choice of rank estimation might be employed, such as an adaptation of the method in [39] to non-Gaussian noise. We note too that rank estimation in spiked models has been the subject of recent investigations [15, 13].

Because the matrix we denoise in the missing data setting does not have Gaussian noise, we test the accuracy of the predicted parameters values against numerical experiments. For  $p = 500, 1000, 2000, 4000, 8000$  and  $p/n = .8$ , we generated 20,000  $p$ -by- $n$  matrices  $\mathbf{X}$  of rank 1, with singular vectors of constant magnitude entries. We then added a Gaussian noise matrix  $\mathbf{G}$ , and subsampled the matrix  $\mathbf{X} + \mathbf{G}$  using row sampling probabilities linearly spaced between .3 and .7, and linearly-spaced column sampling probabilities with the same range. We whiten the resulting matrix to produce the matrix  $\tilde{\mathbf{Y}} = \mathbf{P}^{-1/2} \mathbf{Y} \mathbf{Q}^{-1/2} = \tilde{\mathbf{X}} + \tilde{\mathbf{G}}$ , where  $\tilde{\mathbf{X}} = \mathbf{P}^{-1/2} \mathcal{F}^*(\mathcal{F}(\mathbf{X})) \mathbf{Q}^{-1/2}$ , and  $\tilde{\mathbf{G}} = \mathbf{P}^{-1/2} \mathbf{N} \mathbf{Q}^{-1/2}$ . Since  $\tilde{\mathbf{X}}$  approaches  $\mathbf{P}^{1/2} \mathbf{X} \mathbf{Q}^{1/2}$  in operator norm, if  $\tilde{\mathbf{G}}$  were Gaussian our theory would predict the cosines between the singular vectors of  $\tilde{\mathbf{Y}}$  and  $\mathbf{P}^{1/2} \mathbf{X} \mathbf{Q}^{1/2}$ . In Table 1, we compare the predicted values to the observed values. We measure the average bias over the 20,000 experiments, and the error, which we define as the square root of the average relative squared difference between the observed and predicted values. We see that the errors decay at approximately the rate  $O(n^{-1/2})$ .

## 6.2 Doubly-heteroscedastic noise

In this experiment, we evaluate the performance of denoising matrices with doubly-heteroscedastic noise, using whitening and weighted singular value denoising. We ran the following experiment. We generated a rank 5 signal matrix  $\mathbf{X}$  of size 1000-by-2000. For a specified  $\kappa \geq 1$ , we generated row and column diagonal covariance matrices  $\mathbf{A}$  and  $\mathbf{B}$ , each with condition number  $\kappa$  with linearly-spaced eigenvalues. We

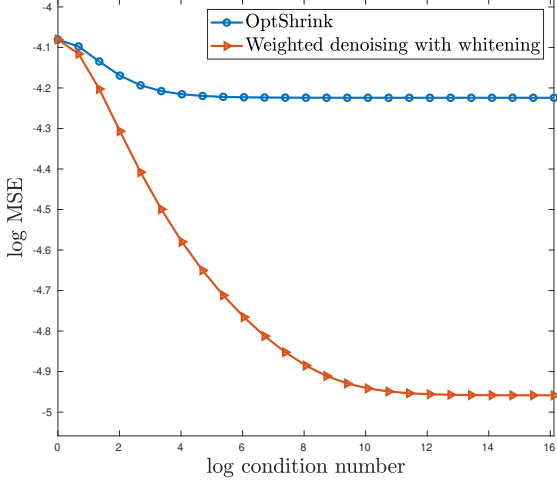


Figure 4: Optimal singular value denoising with bi-whitening versus OptShrink.

then generated the noise matrix  $\mathbf{A}^{1/2}\mathbf{G}\mathbf{B}^{1/2}$ , where  $\mathbf{G}$  has iid Gaussian entries. We observe the matrix  $\mathbf{X} + \mathbf{A}^{1/2}\mathbf{G}\mathbf{B}^{1/2}$ .

For each draw of this data, we perform the denoising scheme based on whitening, weighted singular value denoising, and unwhitening, as described in Section 2.1. We also apply the method of OptShrink [45], which optimally denoises singular values for colored noise matrices (without whitening the noise).

In Figure 4, we plot the errors of these two schemes as a function of the condition number  $\kappa$ . We see that denoising with whitening and weighted singular value denoising outperforms OptShrink, and the improvement increases as the condition number  $\kappa$  grows. This same phenomenon for one-sided heteroscedasticity and one-sided whitening was observed in [41] as well.

### 6.3 Separable denoisers versus least-squares denoisers

In this section, we compare the least-squares denoiser described in Section 4.1 to the separable denoiser from Section 4.2, which assumes the weighted orthogonality condition on  $\mathbf{X}$ 's singular vectors.

We consider the following experimental simple set-up. The coordinates for both rows and columns are split in half; we consider weight functions  $\Omega$  and  $\Pi$  that are 1 on half the coordinates, and 10 on the other half. We generate a rank 2 signal matrix with singular vectors  $\mathbf{u}_1, \mathbf{u}_2$  and  $\mathbf{v}_1, \mathbf{v}_2$ , as follows. We set  $\mathbf{u}_1$  and  $\mathbf{v}_1$  to be constant vectors; and  $\mathbf{u}_2$  and  $\mathbf{v}_2$  are generated as constant on half the coordinates, and a Gaussian with mean  $D > 0$  on the other half; and then orthogonalized to  $\mathbf{u}_1$  and  $\mathbf{v}_1$ , respectively. The larger the “connection” parameter  $D$ , which connects  $\mathbf{u}_1$  and  $\mathbf{u}_2$  (respectively,  $\mathbf{v}_1$  and  $\mathbf{v}_2$ ) on the two subdomains, the larger the variation from the weighted orthogonality assumption.

We then perform denoising using both the least-squares method described in Section 4.1, and the separable method described in Section 4.2. In Figure 5, we plot the errors of these two methods as a function of the connection parameter  $D$ . We see that there is a substantial difference between the two procedures as  $D$  increases, i.e. as the data deviates from weighted orthogonality assumption. This suggests the value in using the least-squares denoiser.

### 6.4 Localized denoising versus global shrinkage

In this experiment, we illustrate the theoretical results from Section 5, comparing localized denoising other procedures. In the first test, we compare localized denoising to global singular value shrinkage. We generate a 500-by-1000 rank 3 signal matrix  $\mathbf{X}$  with singular vectors  $\mathbf{u}_1, \mathbf{u}_2, \mathbf{u}_3$  and  $\mathbf{v}_1, \mathbf{v}_2, \mathbf{v}_3$  as follows: before unit normalization, the coordinates are independent Gaussians, with half the coordinates having variance 1, and the other half having variance  $R^2$ , for a given parameter  $R \geq 1$  representing the ratio of energy between the two components. We add iid Gaussian noise  $G$  to  $\mathbf{X}$  to form the observed matrix  $\mathbf{Y} = \mathbf{X} + \mathbf{G}$ .

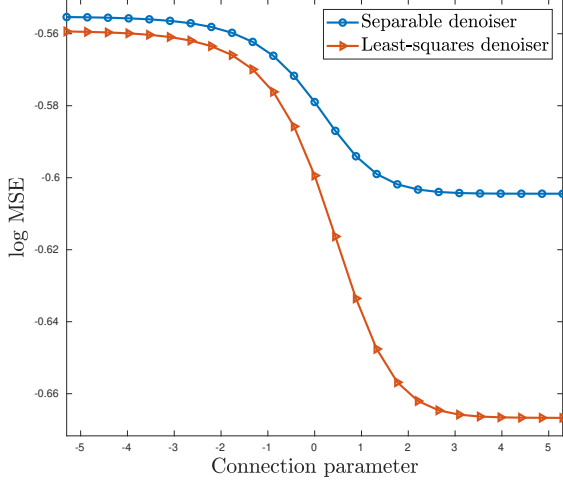


Figure 5: The least-squares denoiser versus separable denoiser.

We perform localized denoising by tiling the matrix into its four submatrices. We also perform global singular value shrinkage to the whole matrix. We run the experiment 40 times. In the left panel of Figure 6, we plot the errors as a function of the ratio  $R$ . As is apparent from the plot, localized denoising is always better than global shrinkage, and its relative performance improves as the signal matrix's singular vectors become more heterogeneous.

The next experiment is concerned with denoising a submatrix  $\mathbf{X}_0$  of  $\mathbf{X}$ , as in Section 5.3. Proposition 5.3 predicts that so long as the singular vectors are not too concentrated on  $\mathbf{X}_0$ , localized denoising will outperform shrinking  $\mathbf{Y}_0$  directly. In the right panel of Figure 6, we show the errors in denoising  $\mathbf{X}_0$  using localized denoising of the whole matrix  $\mathbf{Y}$  and using singular shrinkage applied to  $\mathbf{Y}_0$  alone, as a function of the ratio  $R$ . As we see, once  $R$  exceeds a certain threshold – that is, when the signal on  $\mathbf{X}_0$  is sufficiently strong – then shrinking  $\mathbf{Y}_0$  alone performs better. However, when the signal is not too concentrated on  $\mathbf{X}_0$ , we do a better job denoising  $\mathbf{X}_0$  by using localized denoising on the whole matrix  $\mathbf{Y}$ , as predicted by Proposition 5.3.

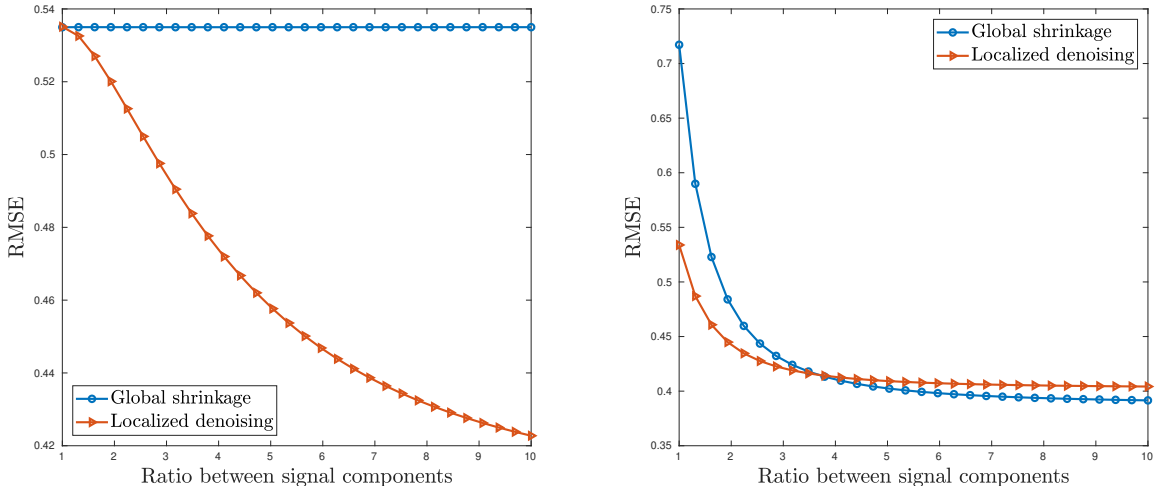


Figure 6: Localized denoising versus global shrinkage. Left: denoising the entire matrix  $\mathbf{X}$ . Right: denoising a submatrix  $\mathbf{X}_0$ .

## 7 Conclusion

This paper has introduced optimal spectral denoisers for weighted loss functions, extending the results of [41]. By judiciously combining these denoisers, we derived a method for matrix denoising that is strictly better than global singular value shrinkage for heterogeneous signals.

The theory we have developed holds for Gaussian noise matrices  $\mathbf{G}$ . However, one of the proposed applications of our theory is to problems with missing data — and more generally, the linearly-transformed spiked model described in [14] — for which the noise term is typically not Gaussian. While numerical simulations show agreement with the predicted theory even for non-Gaussian noise, an open question is to extend our theoretical results to these more general noise models. This will allow us to justify the use of our denoisers for the linearly-transformed spiked model.

Future work will also apply our optimal denoisers to problems where suboptimal spectral denoisers have been employed, as in [7]. More speculatively, we anticipate potential applications of the material in Section 5 to problems in which datasets are drawn from different experimental regimes, as is known to occur in genetic microarray experiments [30, 42, 49], single-cell RNA processing [51, 55], and medical imaging (due, for example, to differences in sample preparation) [38]. In these settings, it is known a priori that signal components are likely to be heterogeneous, and so localized shrinkage is a natural tool.

## Acknowledgements

I thank Edgar Dobriban, Elad Romanov, and Amit Singer for stimulating discussions related to this work. I acknowledge support from the NSF BIGDATA program, IIS 1837992.

## References

- [1] Zhidong Bai and Jian feng Yao. Central limit theorems for eigenvalues in a spiked population model. *Annales de l'Institut Henri Poincaré, Probabilités et Statistiques*, 44(3):447–474, 2008.
- [2] Zhidong Bai and Jian feng Yao. On sample eigenvalues in a generalized spiked population model. *Journal of Multivariate Analysis*, 106:167–177, 2012.
- [3] Zhidong Bai and Jack W. Silverstein. *Spectral analysis of large dimensional random matrices*. Springer Series in Statistics. Springer, 2009.
- [4] Jinho Baik and Jack W. Silverstein. Eigenvalues of large sample covariance matrices of spiked population models. *Journal of Multivariate Analysis*, 97(6):1382–1408, 2006.
- [5] Florent Benaych-Georges, Alice Guionnet, and Mylène Maida. Fluctuations of the extreme eigenvalues of finite rank deformations of random matrices. *Electronic Journal of Probability*, 16:1621–1662, 2011.
- [6] Florent Benaych-Georges and Raj Rao Nadakuditi. The singular values and vectors of low rank perturbations of large rectangular random matrices. *Journal of Multivariate Analysis*, 111:120–135, 2012.
- [7] Tejal Bhamre, Teng Zhang, and Amit Singer. Denoising and covariance estimation of single particle cryo-EM images. *Journal of Structural Biology*, 195(1):72–81, 2016.
- [8] Stephen Boyd and Lieven Vandenberghe. *Convex Optimization*. Cambridge University Press, 2004.
- [9] Emmanuel J. Candès and Yaniv Plan. Matrix completion with noise. *Proceedings of the IEEE*, 98(6):925–936, 2010.
- [10] Emmanuel J. Candès and Terence Tao. The power of convex relaxation: Near-optimal matrix completion. *IEEE Transactions on Information Theory*, 56(5):2053–2080, 2010.
- [11] Yudong Chen, Srinadh Bhojanapalli, Sujay Sanghavi, and Rachel Ward. Completing any low-rank matrix, provably. *The Journal of Machine Learning Research*, 16(1):2999–2034, 2015.

[12] Emilio Gómez Déniz. On the use of the weighted balanced loss function to obtain credibility premiums. In *International Conference on Mathematical and Statistical Modeling in Honor of Enrique Castillo*, 2006.

[13] Edgar Dobriban. Permutation methods for factor analysis and PCA. *arXiv preprint arXiv:1710.00479*, 2017.

[14] Edgar Dobriban, William Leeb, and Amit Singer. Optimal prediction in the linearly transformed spiked model. *arXiv preprint arXiv:1709.03393*, 2017.

[15] Edgar Dobriban and Art B. Owen. Deterministic parallel analysis: an improved method for selecting factors and principal components. *Journal of the Royal Statistical Society: Series B (Statistical Methodology)*, 2018.

[16] David A. Freedman and Richard A. Berk. Weighting regressions by propensity scores. *Evaluation Review*, 32(4):392–409, 2008.

[17] Matan Gavish and David L. Donoho. Minimax risk of matrix denoising by singular value thresholding. *The Annals of Statistics*, 42(6):2413–2440, 2014.

[18] Matan Gavish and David L. Donoho. The optimal hard threshold for singular values is  $4/\sqrt{3}$ . *IEEE Transactions on Information Theory*, 60(8):5040–5053, 2014.

[19] Matan Gavish and David L. Donoho. Optimal shrinkage of singular values. *IEEE Transactions on Information Theory*, 63(4):2137–2152, 2017.

[20] Gene H. Golub and Charles F. Van Loan. *Matrix Computations*, volume 3. JHU Press, 2012.

[21] John C. Gower and Garmt B. Dijksterhuis. *Procrustes Problems*, volume 30. Oxford University Press on Demand, 2004.

[22] Walid Hachem, Philippe Loubaton, and Jamal Najim. Deterministic equivalents for certain functionals of large random matrices. *The Annals of Applied Probability*, 17(3):875–930, 2007.

[23] Walid Hachem, Philippe Loubaton, and Jamal Najim. A CLT for information-theoretic statistics of gram random matrices with a given variance profile. *The Annals of Applied Probability*, 18(6):2071–2130, 2008.

[24] David Lee Hanson and Farroll Tim Wright. A bound on tail probabilities for quadratic forms in independent random variables. *The Annals of Mathematical Statistics*, 42(3):1079–1083, 1971.

[25] David Hong, Laura Balzano, and Jeffrey A. Fessler. Towards a theoretical analysis of PCA for heteroscedastic data. In *54th Annual Allerton Conference on Communication, Control, and Computing*, pages 496–503. IEEE, 2016.

[26] David Hong, Laura Balzano, and Jeffrey A. Fessler. Asymptotic performance of PCA for high-dimensional heteroscedastic data. *Journal of Multivariate Analysis*, 2018.

[27] David Hong, Laura Balzano, and Jeffrey A. Fessler. Optimally Weighted PCA for High-Dimensional Heteroscedastic Data. *arXiv preprint arXiv:1810.12862*, 2018.

[28] Prateek Jain, Praneeth Netrapalli, and Sujay Sanghavi. Low-rank matrix completion using alternating minimization. In *Proceedings of the Forty-fifth Annual ACM Symposium on Theory of Computing*, pages 665–674. ACM, 2013.

[29] Shuiwang Ji and Jieping Ye. An accelerated gradient method for trace norm minimization. In *Proceedings of the 26th Annual International Conference on Machine Learning*, pages 457–464. ACM, June 2009.

[30] W. Evan Johnson, Cheng Li, and Ariel Rabinovic. Adjusting batch effects in microarray expression data using empirical Bayes methods. *Biostatistics*, 8(1), 2007.

[31] Iain M Johnstone. On the distribution of the largest eigenvalue in principal components analysis. *Annals of Statistics*, 29(2):295–327, 2001.

[32] Raghunandan H. Keshavan and Andrea Montanari. Regularization for matrix completion. In *Proceedings of International Symposium on Information Theory*, pages 1503–1507. IEEE, 2010.

[33] Raghunandan H Keshavan, Andrea Montanari, and Sewoong Oh. Matrix completion from a few entries. *IEEE Transactions on Information Theory*, 56(6):2980–2998, 2010.

[34] Faisal Khan, Hangzhou Wang, and Ming Yang. Application of loss functions in process economic risk assessment. *Chemical Engineering Research and Design*, 111, 2016.

[35] Olga Klopp. Noisy low-rank matrix completion with general sampling distribution. *Bernoulli*, 20(1):282–303, 2014.

[36] Vladimir Koltchinskii, Karim Lounici, and Alexandre B Tsybakov. Nuclear-norm penalization and optimal rates for noisy low-rank matrix completion. *The Annals of Statistics*, pages 2302–2329, 2011.

[37] Martin A. Koschat and Deborah F. Swayne. A weighted Procrustes criterion. *Psychometrika*, 56(2):229–239, 1991.

[38] Sonal Kothari, John H. Phan, Richard A. Moffitt, Todd H. Stokes, Shelby E. Hassberger, Qaiser Chaudry, Andrew N. Young, and May D. Wang. Automatic batch-invariant color segmentation of histological cancer images. In *IEEE International Symposium on Biomedical Imaging: From Nano to Macro*, pages 657–660. IEEE, 2011.

[39] Shira Krutchman and Boaz Nadler. Non-parametric detection of the number of signals: Hypothesis testing and random matrix theory. *IEEE Transactions on Signal Processing*, 57(10):3930–3941, 2009.

[40] Alex Kulesza, Nan Jiang, and Satinder Singh. Low-rank spectral learning with weighted loss functions. In *Proceedings of the Eighteenth International Conference on Artificial Intelligence and Statistics*, pages 517–525, 2015.

[41] William Leeb and Elad Romanov. Optimal spectral denoising and PCA with heteroscedastic noise. *arXiv preprint arXiv:1811.02201v2*, 2019.

[42] Jeffrey T. Leek, Robert B. Scharpf, Héctor Corrada Bravo, Benjamin Langmead David Simcha, W. Evan Johnson, Donald Geman, Keith Baggerly, and Rafael A. Irizarry. Tackling the widespread and critical impact of batch effects in high-throughput data. *Nature Reviews Genetics*, 11(10), 2010.

[43] Robert W. Lissitz, Peter H. Schönemann, and James C. Lingoes. A solution to the weighted Procrustes problem in which the transformation is in agreement with the loss function. *Psychometrika*, 41(4):547–550, 1976.

[44] Lydia T. Liu, Edgar Dobriban, and Amit Singer. ePCA: High dimensional exponential family PCA. *The Annals of Applied Statistics*, 12(4):2121–2150, 2018.

[45] Raj Rao Nadakuditi. Optshrink: An algorithm for improved low-rank signal matrix denoising by optimal, data-driven singular value shrinkage. *IEEE Transactions on Information Theory*, 60(5):3002–3018, 2014.

[46] Debasish Paul. Asymptotics of sample eigenstructure for a large dimensional spiked covariance model. *Statistica Sinica*, 17(4):1617–1642, 2007.

[47] Benjamin Recht. A simpler approach to matrix completion. *Journal of Machine Learning Research*, 12:3413–3430, December 2011.

[48] Mark Rudelson and Roman Vershynin. Hanson-Wright inequality and sub-gaussian concentration. *Electronic Communications in Probability*, 18, 2013.

- [49] Andreas Scherer. *Batch Effects and Noise in Microarray Experiments: Sources and Solutions*, volume 868. John Wiley & Sons, 2009.
- [50] Andrey A. Shabalin and Andrew B. Nobel. Reconstruction of a low-rank matrix in the presence of Gaussian noise. *Journal of Multivariate Analysis*, 118:67–76, 2013.
- [51] Uri Shaham, Kelly P. Stanton, Jun Zhao, Huamin Li, Khadir Raddassi, Ruth Montgomery, and Yuval Kluger. Removal of batch effects using distribution-matching residual networks. *Bioinformatics*, 33(16):2539–2546, 2017.
- [52] Nathan Srebro and Tommi Jaakkola. Weighted low-rank approximations. In *Proceedings of the 20th International Conference on Machine Learning*, pages 720–727, 2003.
- [53] Terence Tao. *Topics in random matrix theory*, volume 132. American Mathematical Society, 2012.
- [54] Luis Torgo and Rita Ribeiro. Utility-based regression. In *European Conference on Principles of Data Mining and Knowledge Discovery*, pages 597–604. Springer, 2007.
- [55] Po-Yuan Tung, John D. Blischak, Chiaowen Joyce Hsiao, David A. Knowles, Jonathan E. Burnett, Jonathan K. Pritchard, and Yoav Gilad. Batch effects and the effective design of single-cell gene expression studies. *Scientific Reports*, 7(39921), 2017.
- [56] Roman Vershynin. Introduction to the non-asymptotic analysis of random matrices. *arXiv preprint arXiv:1011.3027*, 2010.
- [57] Farroll Tim Wright. A bound on tail probabilities for quadratic forms in independent random variables whose distributions are not necessarily symmetric. *The Annals of Probability*, 1(6):1068–1070, 1973.
- [58] Anru Zhang, T. Tony Cai, and Yihong Wu. Heteroskedastic PCA: Algorithm, optimality, and applications. *arXiv preprint arXiv:1810.08316*, 2018.